Analytical representations of the spread harmonic measure density

Denis S. Grebenkov*

Laboratoire de Physique de la Matière Condensée (UMR 7643), CNRS–Ecole Polytechnique, 91128 Palaiseau, France
and St. Petersburg National Research University of Information Technologies, Mechanics and Optics, 197101 St. Petersburg, Russia

(Received 27 January 2015; published 7 May 2015)

We study the spread harmonic measure that characterizes the spatial distribution of reaction events on a partially reactive surface. For Euclidean domains in which Brownian motion can be split into independent lateral and transverse displacements, we derive analytical formulas for the spread harmonic measure density and analyze its asymptotic behavior. This analysis is applicable to slab domains, general cylindrical domains, and a half-space. We investigate the spreading effect due to multiple reflections on the surface, and the underlying role of finite reactivity. We discuss further extensions and applications of analytical results to describe Laplacian transfer phenomena such as permeation through semipermeable membranes, secondary current distribution on partially blocking electrodes, and surface relaxation in nuclear magnetic resonance.

DOI: 10.1103/PhysRevE.91.052108 PACS number(s): 02.50.−r, 05.60.−k, 05.10.−a, 02.70.Rr

I. INTRODUCTION

In many physical, chemical, and biological systems, particles diffuse in the bulk toward specific sites located on a reactive surface. Examples can be found in heterogeneous catalysis (when a reactant has to reach a catalytic site on a catalyst's surface to initiate its chemical transformation [1–9]), in living cells (when enzymes search for specific DNA sequences to start replication or another biochemical process [10–17]), and in nuclear magnetic resonance (when excited nuclei relax their magnetization on paramagnetic impurities dispersed on a solid wall of a porous medium [18–25]). These diffusion-reaction processes present a class of first-passage phenomena, in which the reaction event is often characterized by an appropriate first-passage time [26–28]. Depending on the problem, it can describe the first time of arrival onto the reactive surface, the moment of reaction, relaxation or replication on the surface, or the escape time from the confining domain. Similar equations appear in the mathematical description of partially blocking electrodes in electrochemistry [29–37].

The complementary information about the diffusion-reaction process can be gained by studying the spatial distribution of reaction events. For this purpose, one can introduce a measure $\omega_{\mathbf{x}_0}\{A\}$ defined as the probability for reaction to happen on a subset A of the reactive surface when the particle has started from a bulk point $\mathbf{x}_0$. The most known example is the harmonic measure that characterizes the probability that the first arrival onto the surface occurs on the subset A [38]. For a Euclidean domain Ω, the harmonic measure, as a function of the starting point $\mathbf{x}_0$, satisfies the Laplace equation,

$$\Delta\omega_{\mathbf{x}_0}\{A\} = 0 \quad (\mathbf{x}_0 \in \Omega) \tag{1}$$

for any subset A of the boundary $\partial\Omega$ of Ω.[1] This equation is complemented by the Dirichlet boundary condition on $\partial\Omega$:

$$\omega_{\mathbf{x}_0}\{A\} = \mathbb{I}_A(\mathbf{x}_0) \quad (\mathbf{x}_0 \in \partial\Omega), \tag{2}$$

where $\mathbb{I}_A(\mathbf{x}_0)$ is the indicator function of A: $\mathbb{I}_A(\mathbf{x}_0) = 1$ if $\mathbf{x}_0 \in A$, and 0 otherwise. The harmonic measure has numerous applications by determining, e.g., the growth rates in diffusion-limited aggregation, primary current distribution in electrochemistry, distribution of particle fluxes on a membrane, and electric charge distribution on a metallic surface [39–42]. In particular, $\omega_{\mathbf{x}_0}\{A\}$ can be interpreted as a fraction of surface charge induced on a subset A of the grounded conducting surface $\partial\Omega$ by a point charge at $\mathbf{x}_0$ [43]. Scaling behavior and multifractal properties of the harmonic measure on irregular boundaries were thoroughly investigated [44–51].

While the harmonic measure characterizes the first arrival onto the boundary, reaction events may not happen immediately upon the arrival (Fig. 1). In fact, most realistic models of physical, chemical, and biological boundary transfer allow for multiple reflections on the surface before reaction [1,3,34–37,52–55]. In the simplest situation, the particle that hit the surface can either react with a prescribed absorption probability, p, or be rebounced to resume its bulk diffusion until the next arrival. These multiple reflections can be caused by different microscopic mechanisms, such as finite permeability of a membrane, finite reactivity of a catalytic surface, or finite relaxivity of a solid wall. In addition, they can model the effect of a heterogeneous distribution of reactive sites at small length scales (if the particle hits the surface at a passive point, it needs a number of reflections to reach an active point) or the effect of randomly activated gates [when the particle arrives onto the surface, the "gate" at the arrival point can be either active (open) or passive (closed), and the particle is reflected in the latter case].

When the absorption probability is homogeneous in time and space, while reflections have no memory and are independent of particle diffusion, the random number of reflections prior to reaction follows the geometric probability distribution characterized by the absorption probability p. For a continuous formulation, it is convenient to consider the renormalized number of reflections or, equivalently, the local time process on the boundary [56,57],

$$\ell_t = \lim_{a\to 0} a\mathcal{N}_t(a), \tag{3}$$

*denis.grebenkov@polytechnique.edu

[1]Strictly speaking, a measure is defined for any subset A from the Borel σ-algebra of subsets of the boundary; see [38].

 ©2015 American Physical Society

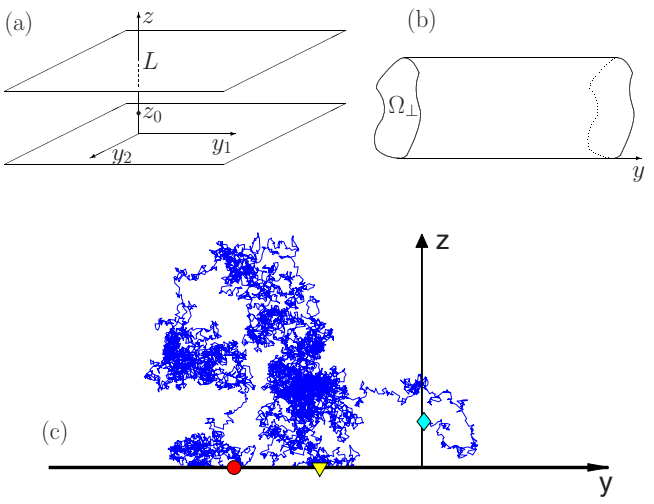

FIG. 1. (Color online) (a) Slab $\Omega = \mathbb{R}^2 \times [0,L]$ and (b) cylinder $\Omega = \mathbb{R} \times \Omega_\perp$ of arbitrary cross section $\Omega_\perp$ as examples of domains for which Brownian motion can be split into independent lateral and transverse displacements. (c) Simulated partially reflected Brownian motion in the half-plane $\Omega = \mathbb{R} \times \mathbb{R}_+$. The diamond, triangle, and circle show the starting point at $\mathbf{x}_0 = (0,z_0)$, the first arrival point onto the horizontal line (reactive surface), and the stopping position, respectively.

where $\mathcal{N}_t(a)$ is the (random) number of passages of reflected Brownian motion through a boundary layer of width a up to time t (here, the use of a finite width a is necessary because after the first hit, reflected Brownian motion returns to the surface infinitely many times during an arbitrarily short period). The reaction occurs at the stopping time τ when the local time process ℓ_t exceeds an independent exponentially distributed random variable ζ characterized by a length Λ [52]:

$$\tau = \inf\{t > 0 : \ell_t > \zeta\}, \quad \mathbb{P}\{\zeta > z\} = \exp(-z/\Lambda). \tag{4}$$

Since ℓ_t can be interpreted as the total distance traveled by reflected Brownian motion in the transverse direction in a vicinity of the boundary, the length Λ appears as the mean traveled distance. This length is naturally related to both macroscopic transport parameters ($\Lambda = D/\kappa$, where D is the bulk diffusion coefficient and κ is the permeability, reactivity, or relaxivity of the surface) and microscopic parameters [$\Lambda = a(1-p)/p$, where a is the reflection distance in a discretized model]. The resulting diffusive process conditioned to stop at the random time τ was called the partially reflected Brownian motion [52].

The spatial distribution of the stopping points (reaction events) can be characterized by the so-called spread harmonic measure, $\omega^\Lambda_{\mathbf{x}_0}\{A\}$, i.e., the probability that the stopping point belongs to a subset A of the boundary. As a function of the starting point $\mathbf{x}_0$, the spread harmonic measure satisfies the Laplace equation (1) with the Robin boundary condition [52]:

$$\left[\omega^\Lambda_{\mathbf{x}_0}\{A\} + \Lambda \frac{\partial}{\partial n}\omega^\Lambda_{\mathbf{x}_0}\{A\}\right] = \mathbb{I}_A(\mathbf{x}_0) \quad (\mathbf{x}_0 \in \partial\Omega), \tag{5}$$

where $\partial/\partial n$ is the normal derivative oriented outward the domain Ω.[2] The presence of the derivative in the second term requires certain smoothness restrictions on the boundary (see [52] for details). Setting $\Lambda = 0$ (i.e., $\kappa = \infty$ or $p = 1$), one retrieves the harmonic measure.

Scaling properties of the spread harmonic measure on prefractal boundaries, the spreading effect due to multiple reflections, and the relation to the Dirichlet-to-Neumann operator have been studied [52,58,59]. In particular, the spread harmonic measure naturally appears in the description of the Laplacian transfer [37,60]. When the boundary is smooth, the spread harmonic measure is fully characterized by its density $\omega^\Lambda_{\mathbf{x}_0}(\mathbf{s})$:

$$\omega^\Lambda_{\mathbf{x}_0}\{A\} = \int_A d\mathbf{s}\, \omega^\Lambda_{\mathbf{x}_0}(\mathbf{s}). \tag{6}$$

In this paper, we aim at deriving analytical representations of the spread harmonic measure density $\omega^\Lambda_{\mathbf{x}_0}(\mathbf{s})$ for a class of Euclidean domains that can be represented as a Cartesian product: $\Omega = \Omega_{||} \times \Omega_\perp \subset \mathbb{R}^{d+d_\perp}$. In other words, the lateral displacements of Brownian motion in $\Omega_{||}$ are independent of its transverse displacements in $\Omega_\perp$ (Fig. 1). The most common examples of practical interest are the half-space $\mathbb{R}^d \times \mathbb{R}_+$, a slab domain $\mathbb{R}^d \times [0,L]$ between two parallel hyperplanes at distance L, and a cylinder $\mathbb{R} \times \Omega_\perp$ of arbitrary cross section $\Omega_\perp$. We are interested in the probability density $\omega^\Lambda_{\mathbf{x}_0}(\mathbf{y})$ of the stopping position $\mathbf{y} \in \Omega_{||}$ of the lateral component for the diffusive process started from $\mathbf{x}_0 \in \Omega$. The stopping criterion will be determined by the transverse diffusion and related to the statistics of multiple reflections on the surface $\Omega_{||} \times \partial\Omega_\perp$ in order to get the spread harmonic measure (here we assume that $\partial\Omega_\perp \neq \emptyset$, i.e., $\Omega_\perp \neq \mathbb{R}^{d_\perp}$).

The paper is organized as follows. In Sec. II, we first describe a general derivation and then focus on the case of a slab domain $\mathbb{R}^d \times [0,L]$ for which different representations of the spread harmonic measure density are derived and illustrated. The limiting cases of the half-space ($L \to \infty$) and of the harmonic measure ($\Lambda \to 0$) are discussed in detail. Section III presents various extensions and applications of these analytical results.

II. ANALYTICAL FORMULAS

This section presents numerous analytical formulas for the spread harmonic measure density and related objects. Although most of these formulas look rather cumbersome (integrals or infinite series involving Bessel functions), they are well suited for both analytical and numerical computations. To guide a reader through this section, we summarize the main results as follows: (i) for all studied domains in which lateral and transverse displacements are independent, the probability density of stopping points, $\omega_{\mathbf{x}_0}(\mathbf{y})$, is given by Eq. (11); (ii) for unrestricted lateral motion ($\Omega_{||} = \mathbb{R}^d$), the density $\omega_{\mathbf{x}_0}(\mathbf{y})$ can be expressed through the Laplace-transformed probability density of the stopping time according to Eq. (14); (iii) for any

[2]Note that in the original definition in Ref. [52], the normal derivative was oriented inward in the domain that yielded the negative sign in front of the second term in Eq. (5).

bounded transverse domain $\Omega_\perp$, the spectral decomposition of the propagator implies the series expansion (20) for $\omega_{\mathbf{x}_0}(\mathbf{y})$; (iv) for a slab of width L (with $\Omega_\perp = [0,L]$), the coefficients of the series (20) are explicitly given by Eq. (33); (v) for a slab, the harmonic measure density $\omega^0_{z_0,L}(\mathbf{y})$ is provided by equivalent relations (37), (40), and (47); (vi) for a half-space ($L = \infty$), the harmonic measure density $\omega^0_{z_0}(\mathbf{y})$ is provided by equivalent relations (41), (44), and (45); this is the rare case when $\omega^0_{z_0}(\mathbf{y})$ has a simple expression (41); (vii) for a slab, the spread harmonic measure density $\omega^\Lambda_{z_0,L}(\mathbf{y})$ is provided by equivalent relations (59), (61), (62), and (63); (viii) for a half-space, the spread harmonic measure density $\omega^\Lambda_{z_0}(\mathbf{y})$ is provided by equivalent relations (66) and (68); (ix) for an infinite cylinder of an arbitrary bounded cross section, the spread harmonic measure density $\omega^\Lambda_{\mathbf{z}_0}(y)$ is given by Eq. (90); and (x) for diffusion outside the infinite circular cylinder, the spread harmonic measure density $\omega^\Lambda_{\mathbf{z}_0}(y)$ is given by Eq. (94).

A. General formulation

We consider Brownian motion in a Euclidean domain $\Omega = \Omega_{||} \times \Omega_\perp \subset \mathbb{R}^{d+d_\perp}$. Since the lateral motion in $\Omega_{||}$ is independent of the transverse motion in $\Omega_\perp$, the diffusion propagator is factored as $G^{||}_t(\mathbf{y}_0,\mathbf{y})G^\perp_t(\mathbf{z}_0,\mathbf{z})$, where the lateral and transverse diffusion propagators describe the probability density of moving from $\mathbf{y}_0$ to $\mathbf{y}$ in $\Omega_{||}$, and from $\mathbf{z}_0$ to $\mathbf{z}$ in $\Omega_\perp$, during time t. Both propagators satisfy the diffusion (or heat) equation subject to the initial condition with Dirac distribution δ [61–63]:

$$\left[\frac{\partial}{\partial t} - D_{||}\Delta_{\mathbf{y}}\right] G^{||}_t(\mathbf{y}_0,\mathbf{y}) = 0,\ G^{||}_0(\mathbf{y}_0,\mathbf{y}) = \delta(\mathbf{y}_0 - \mathbf{y}), \quad (7)$$

$$\left[\frac{\partial}{\partial t} - D_\perp\Delta_{\mathbf{z}}\right] G^\perp_t(\mathbf{z}_0,\mathbf{z}) = 0,\ G^\perp_0(\mathbf{z}_0,\mathbf{z}) = \delta(\mathbf{z}_0 - \mathbf{z}), \quad (8)$$

where $D_{||}$ and $D_\perp$ are the lateral and transverse diffusion coefficients, and $\Delta_{\mathbf{y}}$ and $\Delta_{\mathbf{z}}$ are the Laplace operators. The Robin boundary condition is imposed on a partially reactive boundary $\partial\Omega_\perp$ in order to be able to deduce the spread harmonic measure:

$$G^\perp_t(\mathbf{z}_0,\mathbf{z}) + \Lambda\frac{\partial}{\partial n}G^\perp_t(\mathbf{z}_0,\mathbf{z}) = 0 \quad (\mathbf{z} \in \partial\Omega_\perp), \quad (9)$$

where the parameter Λ can in general be a function of the boundary point (see below).

We formally introduce the stopping time by defining the density $\rho_{\mathbf{z}_0}(t)$ as

$$\rho_{\mathbf{z}_0}(t) = \int_S d\mathbf{s}\left(-D_\perp\frac{\partial}{\partial n}G^\perp_t(\mathbf{z}_0,\mathbf{z})\right)_{\mathbf{z}=\mathbf{s}}, \quad (10)$$

i.e., by integrating the probability flux at the boundary point $\mathbf{s} \in \partial\Omega_\perp$ (the expression in parentheses) over a prescribed "stopping set" $S \subset \partial\Omega_\perp$. For instance, if $\Lambda = 0$ in Eq. (9), the process is stopped after the first arrival of the transverse motion onto S. In Sec. II C, we discuss the choice of the stopping set S to get the spread harmonic measure. In general, the density $\rho_{\mathbf{z}_0}(t)$ is not normalized to 1 because the particle can react on another subset of the boundary (if $S \neq \partial\Omega_\perp$), or even never reach the boundary (e.g., if $\Omega_\perp$ is the exterior of the unit ball in three dimensions, the probability of reaching the surface $\partial\Omega_\perp$ is $1/|\mathbf{z}|$ due to the transient character of Brownian motion). In fact, the integral of $\rho_{\mathbf{z}_0}(t)$ from 0 to infinity gives the probability of stopping at S. Renormalizing $\rho_{\mathbf{z}_0}(t)$ by this probability yields the conditional probability density of the stopping time. With some abuse of language, we will use the term "probability density" for $\rho_{\mathbf{z}_0}(t)$, regardless of its normalization. In each case, a probabilistic interpretation of the related results will be provided.

Since the lateral and transverse motions are independent, the probability density $\omega^\Lambda_{\mathbf{x}_0}(\mathbf{y})$ of the stopping position $\mathbf{y}$ can be expressed as the convolution of $\rho_{\mathbf{z}_0}(t)$ with the lateral diffusion propagator $G^{||}_t(\mathbf{y}_0,\mathbf{y})$,

$$\omega_{\mathbf{x}_0}(\mathbf{y}) = \int_0^\infty dt\ \rho_{\mathbf{z}_0}(t)G^{||}_t(\mathbf{y}_0,\mathbf{y}), \quad (11)$$

where $\mathbf{x}_0 = (\mathbf{y}_0,\mathbf{z}_0) \in \Omega$ is the starting point.

When both domains $\Omega_{||}$ and $\Omega_\perp$ are bounded, both propagators can be expressed through Laplacian eigenfunctions, yielding thus a spectral representation of $\omega_{(\mathbf{y}_0,\mathbf{z}_0)}(\mathbf{y})$. In this paper, we study a different situation when $\Omega_{||}$ or/and $\Omega_\perp$ is unbounded.

B. General cylindrical domains

In this section, we focus on cylindrical domains $\Omega = \mathbb{R}^d \times \Omega_\perp$, where $\Omega_\perp$ is a *bounded* domain with reactive surface $\partial\Omega_\perp$. The lateral motion in $\Omega_{||} = \mathbb{R}^d$ is characterized by the Gaussian propagator

$$G^{||}_t(\mathbf{y}_0,\mathbf{y}) = \frac{1}{(4\pi D_{||}t)^{d/2}}\exp\left(-\frac{|\mathbf{y}-\mathbf{y}_0|^2}{4D_{||}t}\right). \quad (12)$$

Since the lateral motion is translation-invariant, we fix the starting point to be above the origin: $\mathbf{y}_0 = \mathbf{0}$.

Taking the Fourier transform of Eq. (11) with respect to $\mathbf{y}$ and using the Gaussian form of the lateral propagator, one gets the following relation between the Fourier-transformed probability density of the stopping position and the Laplace-transformed probability density of the stopping time:

$$\mathcal{F}_{\mathbf{k}}\{\omega_{\mathbf{z}_0}(\mathbf{y})\} = \int_0^\infty dt\ e^{-D_{||}|\mathbf{k}|^2 t}\rho_{\mathbf{z}_0}(t) \equiv \mathcal{L}_{D_{||}|\mathbf{k}|^2}\{\rho_{\mathbf{z}_0}(t)\}, \quad (13)$$

where $\mathcal{F}_{\mathbf{k}}\{\cdots\}$ and $\mathcal{L}_s\{\cdots\}$ denote the Fourier and Laplace transforms, respectively. The inverse Fourier transform yields the general integral representation:

$$\begin{aligned}\omega_{\mathbf{z}_0}(\mathbf{y}) &= \int_{\mathbb{R}^d}\frac{d\mathbf{k}}{(2\pi)^d}e^{-i(k_1y_1+\cdots k_dy_d)}\mathcal{L}_{D_{||}|\mathbf{k}|^2}\{\rho_{\mathbf{z}_0}(t)\}\\ &= \frac{|\mathbf{y}|^{1-\frac{d}{2}}}{(2\pi)^{\frac{d}{2}}}\int_0^\infty dk\,k^{\frac{d}{2}}J_{\frac{d}{2}-1}(k|\mathbf{y}|)\mathcal{L}_{D_{||}k^2}\{\rho_{\mathbf{z}_0}(t)\}, \quad (14)\end{aligned}$$

where $J_\nu(z)$ is the Bessel function of the first kind, and we used the identity

$$\begin{aligned}&\int_{\mathbb{R}^d}\frac{d\mathbf{k}}{(2\pi)^d}e^{-i(k_1y_1+\cdots+k_dy_d)}f(|\mathbf{k}|)\\ &\quad= \frac{|\mathbf{y}|^{1-\frac{d}{2}}}{(2\pi)^{\frac{d}{2}}}\int_0^\infty dk\,k^{\frac{d}{2}}J_{\frac{d}{2}-1}(k|\mathbf{y}|)f(k), \quad (15)\end{aligned}$$

which is valid for any function f decaying fast enough to ensure the convergence of the integrals. In general, the

Laplace transform of $\rho_{\mathbf{z}_0}(t)$ is easier to get than $\rho_{\mathbf{z}_0}(t)$ itself. In particular, $\mathcal{L}_{D_{||}k^2}\{\rho_{\mathbf{z}_0}(t)\}$ can be written explicitly for many simple domains while $\rho_{\mathbf{z}_0}(t)$ is known only in a form of an infinite series (see below). The convergence of the integral representation (14) and similar expressions derived below, as well as their numerical computation, are discussed in Appendix.

For the transverse motion in a bounded domain $\Omega_\perp$, the propagator $G_t^\perp(\mathbf{z}_0,\mathbf{z})$ admits a spectral representation,

$$G_t^\perp(\mathbf{z}_0,\mathbf{z}) = \sum_{m=1}^{\infty} u_m^*(\mathbf{z}_0)u_m(\mathbf{z})e^{-D_\perp\lambda_m t}, \tag{16}$$

where the asterisk denotes the complex conjugate, and λ_m and $u_m(\mathbf{z})$ are the eigenvalues and eigenfunctions of the Laplace operator in $\Omega_\perp$:

$$\begin{aligned} &\Delta_{\mathbf{z}}u_m(\mathbf{z}) + \lambda_m u_m(\mathbf{z}) = 0 \quad (\mathbf{z}\in\Omega_\perp),\\ &u_m(\mathbf{z}) + \Lambda\frac{\partial}{\partial n}u_m(\mathbf{z}) = 0 \quad (\mathbf{z}\in\partial\Omega_\perp). \end{aligned} \tag{17}$$

The eigenvalues are enumerated by $m = 1,2,\ldots$ and ordered in ascending order: $0 \leqslant \lambda_1 \leqslant \lambda_2 \leqslant \lambda_3 \leqslant \cdots$, while the eigenfunctions are orthogonal and have L^2 normalization:

$$\int_{\Omega_\perp} d\mathbf{z}\, u_m^*(\mathbf{z})u_m(\mathbf{z}) = \begin{cases} 1 & (m = m'),\\ 0 & (m \neq m'). \end{cases}$$

Substituting the spectral representation (16) into Eq. (10), one gets

$$\rho_{\mathbf{z}_0}(t) = D_\perp \sum_{m=1}^{\infty} c_m(\mathbf{z}_0)\exp(-D_\perp\lambda_m t), \tag{18}$$

where

$$c_m(\mathbf{z}_0) = u_m^*(\mathbf{z}_0)\int_S d\mathbf{s}\left(-\frac{\partial u_m(\mathbf{z})}{\partial n}\right)_{\mathbf{z}=\mathbf{s}}. \tag{19}$$

Substituting Eqs. (12) and (18) into Eq. (11) yields

$$\omega_{\mathbf{z}_0}^\Lambda(\mathbf{y}) = \eta^{\frac{d}{2}+1}\frac{|\mathbf{y}|^{1-\frac{d}{2}}}{(2\pi)^{\frac{d}{2}}}\sum_{m=1}^{\infty} c_m(\mathbf{z}_0)\lambda_m^{\frac{d-2}{4}}K_{\frac{d}{2}-1}(\eta\sqrt{\lambda_m}|\mathbf{y}|), \tag{20}$$

where $\eta = \sqrt{D_\perp/D_{||}}$, $K_\nu(z)$ is the modified Bessel function of the second kind, and we used the identity

$$\int_0^\infty dt\,\frac{e^{-at-b/t}}{t^{d/2}} = 2b^{1-\frac{d}{2}}(ab)^{\frac{d-2}{4}}K_{\frac{d}{2}-1}(2\sqrt{ab}). \tag{21}$$

As expected from the rotation invariance of $\Omega_{||} = \mathbb{R}^d$, the density $\omega_{\mathbf{z}_0}^\Lambda(\mathbf{y})$ depends on the distance $|\mathbf{y}|$ between the origin and the stopping point $\mathbf{y}$. The convergence of the series (20) and similar expressions derived below, as well as their numerical computation, are discussed in Appendix.

The probability of stopping at any distance larger than R follows from Eq. (20):

$$\begin{aligned} P_{\mathbf{z}_0}^\Lambda(R) &\equiv \mathbb{P}\{|\mathbf{y}| > R\} = \int_{|\mathbf{y}|>R} d\mathbf{y}\,\omega_{\mathbf{z}_0}^\Lambda(\mathbf{y})\\ &= \frac{(\eta R)^{\frac{d}{2}}}{2^{\frac{d}{2}-1}\Gamma\left(\frac{d}{2}\right)}\sum_{m=1}^{\infty} c_m(\mathbf{z}_0)\lambda_m^{\frac{d}{4}-1}K_{\frac{d}{2}}(\eta\sqrt{\lambda_m}R), \end{aligned} \tag{22}$$

where $\Gamma(z)$ is the gamma function, and we used the identity

$$\frac{d}{dx}[x^\nu K_\nu(x)] = -x^\nu K_{\nu-1}(x). \tag{23}$$

In particular, the probability of stopping on the set S is

$$P_{\mathbf{z}_0}^\Lambda(0) = \int_{\mathbb{R}^d} d\mathbf{y}\,\omega_{\mathbf{z}_0}^\Lambda(\mathbf{y}) = \sum_{m=1}^{\infty}\frac{c_m(\mathbf{z}_0)}{\lambda_m} = \int_0^\infty dt\,\rho_{\mathbf{z}_0}(t), \tag{24}$$

where the last equality relates spatial and temporal properties of the stopping event. As mentioned earlier, this probability can in general be less than 1. To get the conventional normalization by 1, one can consider the conditional probability density $\omega_{\mathbf{z}_0}^\Lambda(\mathbf{y})/P_{\mathbf{z}_0}^\Lambda(0)$.

The compact exploration of the transverse domain $\Omega_\perp$ results in the exponential decay of the density $\omega_{\mathbf{z}_0}^\Lambda(\mathbf{y})$ in Eq. (20) at large $|\mathbf{y}|$ and of the probability $P_{\mathbf{z}_0}^\Lambda(R)$ in Eq. (22) at large R. In fact, the asymptotic formula

$$K_\nu(z) \simeq \sqrt{\frac{\pi}{2z}}e^{-z} \quad (z \gg 1) \tag{25}$$

yields

$$\begin{aligned} \omega_{\mathbf{z}_0}^\Lambda(\mathbf{y}) &\simeq c_1(\mathbf{z}_0)\frac{\eta^{\frac{d+1}{2}}}{2(2\pi|\mathbf{y}|)^{\frac{d-1}{2}}}\lambda_1^{\frac{d-3}{4}}\exp(-\eta\sqrt{\lambda_1}|\mathbf{y}|),\\ P_{\mathbf{z}_0}^\Lambda(R) &\simeq c_1(\mathbf{z}_0)\frac{\sqrt{\pi}}{\Gamma\left(\frac{d}{2}\right)}\left(\frac{\eta R}{2}\right)^{\frac{d-1}{2}}\lambda_1^{\frac{d-5}{4}}\exp(-\eta\sqrt{\lambda_1}R) \end{aligned} \tag{26}$$

for $|\mathbf{y}| \gg (\eta\sqrt{\lambda_1})^{-1}$ and $R \gg (\eta\sqrt{\lambda_1})^{-1}$, respectively. The decay rate is determined by the smallest eigenvalue λ_1.

In the next section, we provide the explicit formulas for computing λ_m and $c_m(\mathbf{z}_0)$ for a slab domain and then investigate the behavior of the density $\omega_{\mathbf{z}_0}^\Lambda(\mathbf{y})$.

C. Probability density of the first exit time

We consider a slab domain $\Omega = \mathbb{R}^d \times [0,L]$ between two parallel reactive hyperplanes $\Gamma_0 = \{(\mathbf{y},0) : \mathbf{y}\in\mathbb{R}^d\}$ and $\Gamma_L = \{(\mathbf{y},L) : \mathbf{y}\in\mathbb{R}^d\}$ separated by distance L. In this case, one needs to compute the eigenvalues and eigenfunctions of the Laplace operator in the interval $[0,L]$ with two boundary conditions:

$$-D_\perp u_m'(0) + \kappa u_m(0) = 0, \quad D_\perp u_m'(L) + \kappa_1 u_m(L) = 0, \tag{27}$$

where two distinct reactivities κ and κ_1 can be imposed at two end points 0 and L. Setting $u_m(z) = e_1\sin(\alpha x/L) + e_2\cos(\alpha x/L)$, one gets $e_2 = e_1\alpha h$ from the left end point (at $z = 0$) and

$$\frac{\tan\alpha}{\alpha} = \frac{h+h_1}{\alpha^2 h h_1 - 1} \tag{28}$$

from the right end point (at $z = L$), where

$$h = \frac{D_\perp}{\kappa L}, \quad h_1 = \frac{D_\perp}{\kappa_1 L}. \tag{29}$$

Denoting α_m $(m = 1,2,\ldots)$ all positive zeros of Eq. (28) in ascending order, one gets $\lambda_m = \alpha_m^2/L^2$, while the remaining

coefficient e_1 is determined by the L^2 normalization of eigenfunctions. One gets, therefore,

$$u_m(z) = \frac{\beta_m}{\sqrt{L}}[\sin(\alpha_m x/L) + h\alpha_m \cos(\alpha_m x/L)], \tag{30}$$

where

$$\beta_m^{-2} = \frac{1}{2}\left[1 + \alpha_m^2 h^2 + (h+h_1)\frac{1+\alpha_m^2 h h_1}{1+\alpha_m^2 h_1^2}\right]. \tag{31}$$

We also note the relation

$$\sin(\alpha_m z_0/L) + h\alpha_m \cos(\alpha_m z_0/L) = \frac{h\alpha_m \sin\left[\alpha_m\left(1-\frac{z_0}{L}\right)\right]}{\sin\alpha_m} \tag{32}$$

that will be used in the following analysis.

Since the boundary of the transverse domain $\Omega_\perp = [0,L]$ consists of two points, $\partial\Omega_\perp = \{0,L\}$, there are only a few choices for the stopping set S. We consider two situations: $S = \{0\}$ (i.e., only reaction events on the hyperplane Γ_0 matter), and $S = \{0,L\}$ (i.e., reaction events on both hyperplanes Γ_0 and Γ_L matter). In the former case,

$$\begin{aligned} c_m(z_0) &= u_m(z_0)\left(\frac{\partial u_m(z)}{\partial z}\right)_{z=0} \\ &= \frac{\alpha_m \beta_m^2}{L^2}[\sin(\alpha_m z_0/L) + h\alpha_m \cos(\alpha_m z_0/L)] \end{aligned} \tag{33}$$

[since $S = \{0\}$, the integral in Eq. (10) over S is reduced to the value of the probability flux at this point]. The resulting probability densities $\rho^{\Lambda}_{z_0,L}(t)$ and $\omega^{\Lambda}_{z_0,L}(\mathbf{y})$ from Eqs. (18) and (20) are not normalized to 1 because the reaction events at the other hyperplane are ignored (note the subscript L that we added to highlight the presence of the second hyperplane at $z = L$). In fact, the probability of stopping at the hyperplane Γ_0 is

$$P^{\Lambda}_{z_0,L}(0) = \frac{1 - z_0/L + h_1}{1 + h + h_1}. \tag{34}$$

It can be found either by summing the series in Eq. (24) or by solving the Laplace equation on the interval $[0,L]$ with the reactive boundary conditions.

In turn, if the reaction is allowed through *both* end points (i.e., $S = \{0,L\}$), one has to replace $c_m(z_0)$ by

$$\begin{aligned} \tilde{c}_m(z_0) &= u_m(z_0)\left[\left(\frac{\partial u_m(z)}{\partial z}\right)_{z=0} - \left(\frac{\partial u_m(z)}{\partial z}\right)_{z=L}\right] \\ &= \frac{\alpha_m \beta_m^2}{L^2}(1 + h\alpha_m \sin\alpha_m - \cos\alpha_m) \\ &\quad \times [\sin(\alpha_m z_0/L) + h\alpha_m \cos(\alpha_m z_0/L)] \end{aligned} \tag{35}$$

(the tilde sign will be used to distinguish the quantities corresponding to this case). As expected, the resulting probability densities $\tilde{\rho}^{\Lambda}_{z_0,L}(t)$ and $\tilde{\omega}^{\Lambda}_{z_0,L}(\mathbf{y})$ are normalized to 1, i.e., $\tilde{P}^{\Lambda}_{z_0,L}(0) = 1$.

In the next subsection, we analyze the behavior of the harmonic measure density, while Sec. II E is devoted to the spread harmonic measure. For convenience, we assume the same diffusion coefficient D for the lateral and transverse motion, $D_\perp = D_\parallel = D$ (i.e., $\eta = 1$), though all results could be obtained in the anisotropic case as well.

D. Harmonic measure

We first consider the simplest case when both reactivities are infinite, $\kappa = \kappa_1 = \infty$, i.e., $\Lambda = \Lambda_1 = 0$ and $h = h_1 = 0$. Equation (28) is reduced to $\sin\alpha_m = 0$, from which $\alpha_m = \pi m$, $\beta_m^2 = 2$, and $c_m(z_0) = 2\pi m \sin(\pi m z_0/L)$, so that

$$\rho^0_{z_0,L}(t) = \frac{D}{L^2}\sum_{m=1}^{\infty} 2\pi m \sin(\pi m z_0/L) e^{-D\pi^2 m^2 t/L^2} \tag{36}$$

and

$$\begin{aligned} \omega^0_{z_0,L}(\mathbf{y}) &= \frac{(2|\mathbf{y}|/L)^{1-\frac{d}{2}}}{L^d}\sum_{m=1}^{\infty} \sin(\pi m z_0/L) m^{\frac{d}{2}} \\ &\quad \times K_{\frac{d}{2}-1}(\pi m|\mathbf{y}|/L). \end{aligned} \tag{37}$$

This is the harmonic measure density, i.e., the probability density of the first arrival on the hyperplane Γ_0 at $\mathbf{y}$ for Brownian motion started from $(0,z_0) \in \Omega$, *without hitting the other hyperplane* Γ_L. In contrast to $\rho^0_{z_0,L}(t)$ describing temporal statistics, the harmonic measure density does not depend on the diffusion coefficient D. In fact, the harmonic measure characterizes the spatial distribution of arrival points, independently of how long the arrival takes. According to Eq. (24), the integral of this density over $\mathbf{y} \in \mathbb{R}^d$ gives the probability of hitting the hyperplane Γ_0 before the hyperplane Γ_L: $P^0_{z_0,L}(0) = 1 - z_0/L$.

If one is interested in the first arrival on either of the hyperplanes (Γ_0 or Γ_L), one uses $\tilde{c}_m(z_0) = 2\pi m[1 - (-1)^m]\sin(\pi m z_0/L)$ instead of $c_m(z_0)$ to get a slightly different expression,

$$\begin{aligned} \tilde{\omega}^0_{z_0,L}(\mathbf{y}) &= \frac{(2|\mathbf{y}|/L)^{1-\frac{d}{2}}}{L^d}\sum_{m=1}^{\infty}[1-(-1)^m] \\ &\quad \times \sin(\pi m z_0/L) m^{\frac{d}{2}} K_{\frac{d}{2}-1}(\pi m|\mathbf{y}|/L). \end{aligned} \tag{38}$$

Since Brownian motion certainly hits one of two hyperplanes, this density is normalized to 1, as expected.

The Poisson summation formula allows one to rewrite the probability density $\rho^0_{z_0,L}(t)$ of the first exit time through the end point 0 as

$$\rho^0_{z_0,L}(t) = \frac{1}{\sqrt{4\pi D t^3}}\sum_{k=-\infty}^{\infty}(z_0 + 2kL)\exp\left(-\frac{(z_0+2kL)^2}{4Dt}\right), \tag{39}$$

from which another representation for the harmonic measure density follows,

$$\omega^0_{z_0,L}(\mathbf{y}) = \sum_{k=-\infty}^{\infty}\omega^0_{z_0+2kL}(\mathbf{y}), \tag{40}$$

where $\omega^0_{z_0}(\mathbf{y})$ is the generalized Cauchy distribution for the harmonic measure density in the half-space (for which we omit the second subscript $L = \infty$):

$$\omega^0_{z_0}(\mathbf{y}) = \frac{\Gamma\left(\frac{d+1}{2}\right)}{\pi^{\frac{d+1}{2}}}\frac{z_0}{\left(z_0^2 + |\mathbf{y}|^2\right)^{\frac{d+1}{2}}}. \tag{41}$$

Note that Eq. (40) could also be obtained by the method of images. In electrostatics, $\omega^0_{z_0}(\mathbf{y})$ describes the surface charge density on the grounded conducting hyperplane Γ_0 induced

by a point charge at height z_0 above the surface [43]. While the equivalent representations (36) and (39) of the probability density $\rho^0_{z_0,L}(t)$ are, respectively, convenient at long and short times, the equivalent representations (37) and (40) are convenient at long and short distances $|\mathbf{y}|/L$, respectively.

Similarly, if the exit from both end points is allowed, the probability density $\tilde{\rho}^0_{z_0,L}(t)$ and the associated harmonic measure density $\tilde{\omega}^0_{z_0,L}(\mathbf{y})$ are

$$\tilde{\rho}^0_{z_0,L}(t) = \frac{1}{\sqrt{4\pi Dt^3}} \sum_{k=-\infty}^{\infty} (-1)^k (z_0 + kL) e^{-(z_0+kL)^2/(4Dt)},$$
$$\tilde{\omega}^0_{z_0,L}(\mathbf{y}) = \sum_{k=-\infty}^{\infty} (-1)^k \omega^0_{z_0+kL}(\mathbf{y}). \tag{42}$$

In the limit $L \to \infty$ (i.e., no barrier), only the term with $k = 0$ in Eq. (40) survives, yielding the generalized Cauchy formula (41), which decays as a power law,

$$\omega^0_{z_0}(\mathbf{y}) \simeq \frac{\Gamma\left(\frac{d+1}{2}\right)}{\pi^{\frac{d+1}{2}}} \frac{z_0}{|\mathbf{y}|^{d+1}} \quad (|\mathbf{y}| \gg z_0), \tag{43}$$

in contrast to the exponential decay (26) in the presence of a barrier ($L < \infty$). Both the exponential and power-law behaviors of the harmonic measure density are illustrated in Fig. 2. When the barrier is relatively far ($L = 20$, circles), the power-law behavior at small $|\mathbf{y}|/L$ switches to the exponential one at large $|\mathbf{y}|/L$.

For completeness, we also provide the representation of the harmonic measure density through the d-dimensional Fourier transform. For the harmonic measure density in the half-space, the Fourier transform of Eq. (41) yields for $z_0 \geqslant 0$

$$\omega^0_{z_0}(\mathbf{y}) = \int_{\mathbb{R}^d} \frac{d\mathbf{k}}{(2\pi)^d} e^{-i(k_1 y_1 + \cdots + k_d y_d)} e^{-z_0|\mathbf{k}|} \tag{44}$$
$$= \frac{|\mathbf{y}|^{1-\frac{d}{2}}}{(2\pi)^{\frac{d}{2}}} \int_0^\infty dk\, k^{\frac{d}{2}} J_{\frac{d}{2}-1}(k|\mathbf{y}|) e^{-z_0 k}, \tag{45}$$

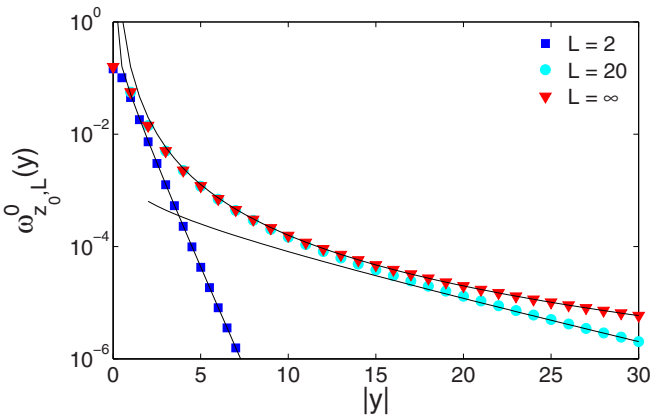

FIG. 2. (Color online) Harmonic measure density $\omega^0_{z_0,L}(\mathbf{y})$ as a function of $|\mathbf{y}|$ for $d = 2$, $z_0 = 1$, and three values of L: 2, 20, and ∞. For $L < \infty$, symbols show the spectral representation (37) while lines indicate the exponential asymptotic decay (26). For $L = \infty$, triangles show the generalized Cauchy distribution (41) while the line indicates the power-law asymptotic decay (43).

where we used the identity (15). Comparing this formula to Eq. (41), one deduces the following relation that will be used below:

$$\int_0^\infty dk\, k^{\frac{d}{2}} J_{\frac{d}{2}-1}(ky) e^{-zk} = \frac{2^{\frac{d}{2}} \Gamma\left(\frac{d+1}{2}\right)}{\sqrt{\pi}\, y^{1-\frac{d}{2}}} \frac{z}{[z^2 + y^2]^{\frac{d+1}{2}}}. \tag{46}$$

Substituting the representation (44) into Eqs. (40) and (42), one can also obtain the Fourier representation for the harmonic measure density in the presence of a barrier:

$$\omega^0_{z_0,L}(\mathbf{y}) = \int_{\mathbb{R}^d} \frac{d\mathbf{k}}{(2\pi)^d} e^{-i(k_1 y_1 + \cdots + k_d y_d)} \frac{\sinh[(L - z_0)|\mathbf{k}|]}{\sinh(L|\mathbf{k}|)}$$
$$= \frac{(|\mathbf{y}|/L)^{1-\frac{d}{2}}}{L^d (2\pi)^{\frac{d}{2}}} \int_0^\infty d\alpha\, \alpha^{\frac{d}{2}} J_{\frac{d}{2}-1}(\alpha|\mathbf{y}|/L) \times \frac{\sinh\left[\alpha\left(1 - \frac{z_0}{L}\right)\right]}{\sinh(\alpha)} \tag{47}$$

and

$$\tilde{\omega}^0_{z_0,L}(\mathbf{y}) = \int_{\mathbb{R}^d} \frac{d\mathbf{k}}{(2\pi)^d} e^{-i(k_1 y_1 + \cdots + k_d y_d)} \frac{\cosh\left[\left(\frac{L}{2} - z_0\right)|\mathbf{k}|\right]}{\cosh\left(\frac{L}{2}|\mathbf{k}|\right)}$$
$$= \frac{(|\mathbf{y}|/L)^{1-\frac{d}{2}}}{L^d (2\pi)^{\frac{d}{2}}} \int_0^\infty d\alpha\, \alpha^{\frac{d}{2}} J_{\frac{d}{2}-1}(\alpha|\mathbf{y}|/L) \times \frac{\cosh\left[\alpha\left(\frac{1}{2} - \frac{z_0}{L}\right)\right]}{\cosh(\alpha/2)}, \tag{48}$$

Given that the poles of the integrand function in Eq. (47) appear at $\alpha = i\pi m$, the spectral representation (37) can be interpreted as the application of the residue theorem to Eq. (47). Comparing Eqs. (44), (47), and (48) to Eq. (14), one can recognize the integrand function as the Laplace transform of the probability density $\rho^0_{z_0,L}(t)$, for instance,

$$\mathcal{L}_s\left\{\rho^0_{z_0,L}(t)\right\} = \frac{\sinh[(L - z_0)\sqrt{s/D}]}{\sinh(L\sqrt{s/D})} \tag{49}$$

for the first exit time from the interval $[0, L]$ through the end point 0 [26].

1. *Two-dimensional stripe*

For a two-dimensional stripe (i.e., $d = 1$), one uses

$$K_{-1/2}(x) = K_{1/2}(x) = \sqrt{\pi/(2x)} e^{-x} \tag{50}$$

to get, after resummation of geometric series,

$$\omega^0_{z_0,L}(y) = \frac{\sin(\pi z_0/L) e^{-\pi|y|/L}}{L[1 - 2\cos(\pi z_0/L) e^{-\pi|y|/L} + e^{-2\pi|y|/L}]}. \tag{51}$$

In the limit $L \to \infty$, one retrieves the Cauchy distribution:

$$\omega^0_{z_0}(y) = \frac{z_0}{\pi\left(z_0^2 + y^2\right)}. \tag{52}$$

Similarly, one gets

$$\tilde{\omega}^0_{z_0,L}(y) = \frac{2\sin(\pi z_0/L) e^{-\pi|y|/L}(1 + e^{-2\pi|y|/L})}{L[1 - 2\cos(2\pi z_0/L) e^{-2\pi|y|/L} + e^{-4\pi|y|/L}]}. \tag{53}$$

2. *Relation to the Green function*

We recall that the harmonic measure density can in general be directly obtained from the Green function of the Laplace operator [64,65]:

$$\omega_{\mathbf{x}_0}(\mathbf{s}) = -\left(\frac{\partial G(\mathbf{x},\mathbf{x}_0)}{\partial n}\right)_{\mathbf{x}=\mathbf{s}}, \tag{54}$$

where $\Delta_{\mathbf{x}} G(\mathbf{x},\mathbf{x}_0) = -\delta(\mathbf{x}-\mathbf{x}_0)$ in Ω and $G(\mathbf{x},\mathbf{x}_0) = 0$ on the boundary of $\partial\Omega$. For the half-space $\mathbb{R}^d \times \mathbb{R}_+$, the Green function with the Dirichlet boundary condition reads

$$G(\mathbf{x},\mathbf{x}_0) = g(\mathbf{x},\mathbf{x}_0) - g(\mathbf{x},\mathbf{x}_0'), \tag{55}$$

where $\mathbf{x}_0' = (\mathbf{y}_0, -z_0)$ is the reflection of $\mathbf{x}_0 = (\mathbf{y}_0, z_0)$ with respect to the hyperplane at $z = 0$, and $g(\mathbf{x},\mathbf{x}_0)$ is the fundamental Green function in the whole space $\mathbb{R}^{d+1}$:

$$g(\mathbf{x},\mathbf{x}_0) = \begin{cases} \dfrac{-1}{2\pi} \ln|\mathbf{x}-\mathbf{x}_0| & (d=1), \\ \dfrac{\Gamma\left(\frac{d-1}{2}\right)}{4\pi^{\frac{d+1}{2}}} \dfrac{1}{|\mathbf{x}-\mathbf{x}_0|^{d-1}} & (d>1). \end{cases} \tag{56}$$

Taking the normal derivative in Eq. (54) yields Eq. (41). In general, the computation of the Green function is not easier than that of the harmonic measure density.

E. Spread harmonic measures

We consider the spread harmonic measure density in a slab domain $\mathbb{R}^d \times [0,L]$. Setting $\kappa_1 = \infty$ (i.e., $\Lambda_1 = h_1 = 0$), Eq. (28) becomes $\tan(\alpha) = -\alpha h$, whose roots α_m belong to $[-\pi/2 + \pi m, \pi m]$ (the extreme cases $h = \infty$ and $h = 0$ correspond to the two ends of this interval). The other expressions are simplified as

$$\beta_m^2 = \frac{2}{1 + h + \alpha_m^2 h^2} \tag{57}$$

and

$$c_m(z_0) = \frac{2\alpha_m[\sin(\alpha_m z_0/L) + h\alpha_m \cos(\alpha_m z_0/L)]}{L^2\left(1 + h + \alpha_m^2 h^2\right)}, \tag{58}$$

whose substitution into Eq. (20) yields the spread harmonic measure density:

$$\omega^{\Lambda}_{z_0,L}(\mathbf{y}) = \frac{(|\mathbf{y}|/L)^{1-\frac{d}{2}}}{L^d(2\pi)^{\frac{d}{2}}} \sum_{m=1}^{\infty} \frac{2h\sin[\alpha_m(1-z_0/L)]}{\left[1 + h + \alpha_m^2 h^2\right]\sin\alpha_m} \times \alpha_m^{\frac{d}{2}} K_{\frac{d}{2}-1}(\alpha_m|\mathbf{y}|/L), \tag{59}$$

where we used Eq. (32). Figure 3(a) illustrates the behavior of this density.

The probability $P^{\Lambda}_{z_0,L}(R)$ from Eq. (22) gets a similar form:

$$P^{\Lambda}_{z_0}(R) = \frac{(R/L)^{\frac{d}{2}}}{2^{\frac{d}{2}-1}\Gamma\left(\frac{d}{2}\right)} \sum_{m=1}^{\infty} \frac{2h\sin[\alpha_m(1-z_0/L)]}{\left[1 + h + \alpha_m^2 h^2\right]\sin\alpha_m} \times \alpha_m^{\frac{d}{2}} K_{\frac{d}{2}}(\alpha_m R/L). \tag{60}$$

In analogy to Eqs. (37) and (47) for the harmonic measure, one can consider Eq. (59) as the result of applying the residue theorem to the following integral:

$$\omega^{\Lambda}_{z_0,L}(\mathbf{y}) = \frac{(|\mathbf{y}|/L)^{1-\frac{d}{2}}}{L^d(2\pi)^{\frac{d}{2}}} \int_0^{\infty} d\alpha \frac{\alpha^{\frac{d}{2}} J_{\frac{d}{2}-1}(\alpha|\mathbf{y}|/L)}{1 + \alpha h\coth(\alpha)} \times \frac{\sinh[\alpha(1-z_0/L)]}{\sinh\alpha}. \tag{61}$$

Using the identity (15), one can also represent the spread harmonic measure density as

$$\omega^{\Lambda}_{z_0,L}(\mathbf{y}) = \int_{\mathbb{R}^d} \frac{d\mathbf{k}}{(2\pi)^d} \frac{e^{-i(k_1 y_1 + \cdots + k_d y_d)}}{1 + \Lambda|\mathbf{k}|\coth(L|\mathbf{k}|)} \times \frac{\sinh[(L-z_0)|\mathbf{k}|]}{\sinh(L|\mathbf{k}|)}. \tag{62}$$

This relation can be seen as the convolution of the harmonic measure density $\omega^0_{z_0,L}(\mathbf{y}_0)$ (describing the first arrival point $\mathbf{y}_0$ onto the boundary) and the transition density $\mathcal{T}^{\Lambda}_L(\mathbf{y}-\mathbf{y}_0) \equiv \omega^{\Lambda}_{0,L}(\mathbf{y}-\mathbf{y}_0)$ (describing the passage from the first arrival point $\mathbf{y}_0$ to the stopping point $\mathbf{y}$):

$$\omega^{\Lambda}_{z_0,L}(\mathbf{y}) = \int_{\mathbb{R}^d} d\mathbf{y}_0 \omega^0_{z_0,L}(\mathbf{y}_0)\mathcal{T}^{\Lambda}_L(\mathbf{y}-\mathbf{y}_0). \tag{63}$$

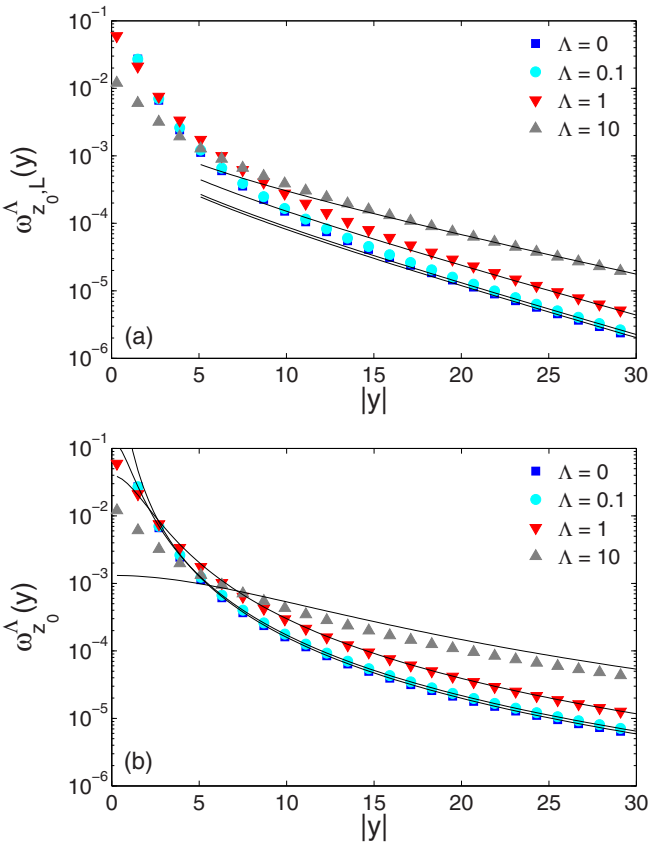

FIG. 3. (Color online) Spread harmonic measure density $\omega^{\Lambda}_{z_0,L}(\mathbf{y})$ as a function of $|\mathbf{y}|$ for $d = 2$, $z_0 = 1$, and four values of Λ: $\{0, 0.1, 1, 10\}$, with a barrier at $L = 20$ (a) and without a barrier (b). For $L = 20$, symbols show the spectral representation (59) while lines indicate the asymptotic relation (26). For $L = \infty$, symbols show the result of numerical integration of Eq. (68) and the approximation (70).

In probabilistic terms, this representation is a consequence of the Markov property of partially reflected Brownian motion: the paths before and after the first arrival are independent. Earlier studies of the spread harmonic measure were mainly focused on $\mathcal{T}_L^\Lambda(\mathbf{y}-\mathbf{y}_0)$, which fully includes the spreading effect [52,58,59]. Setting $z_0=0$ into Eqs. (59), (61), and (62) yields analytical formulas for this kernel. Comparing Eq. (62) to Eq. (14), one can recognize the integrand function as the Laplace transform of $\rho^\Lambda_{z_0,L}(t)$ for a slab domain:

$$\mathcal{L}_s\{\rho^\Lambda_{z_0,L}(t)\}=\frac{\sinh[(L-z_0)\sqrt{s/D}]}{\sinh(L\sqrt{s/D})+\Lambda\sqrt{s/D}\cosh(L\sqrt{s/D})}. \tag{64}$$

From Eq. (61), one deduces an integral representation for the probability $P^\Lambda_{z_0,L}(R)$,

$$P^\Lambda_{z_0,L}(R)=\frac{1-z_0/L}{1+h}-\frac{2[R/(2L)]^{\frac{d}{2}}}{\Gamma(\frac{d}{2})}\times\int_0^\infty d\alpha\,\alpha^{\frac{d}{2}-1}J_{\frac{d}{2}}(\alpha R/L)\times\frac{\sinh[\alpha(1-z_0/L)]}{\sinh\alpha+\alpha h\cosh\alpha} \tag{65}$$

[here, it is convenient to compute first the probability $\mathbb{P}\{|\mathbf{y}|<R\}$ and then to get $\mathbb{P}\{|\mathbf{y}|>R\}$, bearing in mind that the probability of stopping at the hyperplane Γ_0 is $(1-z_0/L)/(1+h)$ according to Eq. (24)].

1. No barrier limit

To obtain the spread harmonic measure density without a barrier (i.e., for a half-space), one can take the limit $L\to\infty$ in Eqs. (61) and (65) to get

$$\omega^\Lambda_{z_0}(\mathbf{y})=\frac{(|\mathbf{y}|/\Lambda)^{1-\frac{d}{2}}}{\Lambda^d(2\pi)^{\frac{d}{2}}}\int_0^\infty d\alpha\,\frac{\alpha^{\frac{d}{2}}J_{\frac{d}{2}-1}(\frac{\alpha|\mathbf{y}|}{\Lambda})e^{-\alpha z_0/\Lambda}}{1+\alpha}, \tag{66}$$

$$P^\Lambda_{z_0}(R)=1-\frac{2^{1-\frac{d}{2}}}{\Gamma(\frac{d}{2})}\int_0^\infty dx\,x^{\frac{d}{2}-1}J_{\frac{d}{2}}(x)\frac{e^{-xz_0/R}}{1+x\Lambda/R}. \tag{67}$$

In the half-space, the harmonic and spread harmonic measures can be related in a particularly simple way. For this purpose, one multiplies the relation (46) by $e^{-z/\Lambda}$, integrates both parts over z from z_0 to infinity, and, after simplifications, identifies the left-hand side with Eq. (66), from which

$$\omega^\Lambda_{z_0}(\mathbf{y})=\frac{\Gamma(\frac{d+1}{2})}{\Lambda\pi^{\frac{d+1}{2}}}\int_0^\infty dz\,\frac{(z+z_0)e^{-z/\Lambda}}{[(z+z_0)^2+|\mathbf{y}|^2]^{\frac{d+1}{2}}}$$

or, equivalently,

$$\omega^\Lambda_{z_0}(\mathbf{y})=\int_0^\infty dz\,\omega^0_{z_0+z}(\mathbf{y})\frac{e^{-z/\Lambda}}{\Lambda}. \tag{68}$$

According to this relation, the spread harmonic measure density can be seen as the Laplace transform of the harmonic measure density $\omega^0_{z_0+z}(\mathbf{y})$ with respect to z. At the same time, this relation appears as the average of the harmonic measure density $\omega^0_{z_0+\zeta}(\mathbf{y})$ over the random height $z_0+\zeta$ above the hyperplane, where ζ follows the exponential law in Eq. (4). Since the local time process ℓ_t in Eq. (3) can be interpreted as the distance traveled by reflected Brownian motion near the boundary and the process is stopped when $\ell_t=\zeta$, the spreading effect is equivalent to starting from a further point $z_0+\zeta$ (or $z_0+\ell_t$). In other words, if the particle traveled the distance z_0 before stopping at a fully reactive boundary ($\Lambda=0$), it would travel the random distance $z_0+\zeta$ before stopping at a partially reactive boundary. Note also that the same convolution structure is applicable to the stopping time, namely,

$$\rho^\Lambda_{z_0}(t)=\int_0^\infty dz\,\rho^0_{z_0+z}(t)\frac{e^{-z/\Lambda}}{\Lambda}. \tag{69}$$

Integrating Eq. (68) by parts twice, one deduces the asymptotic behavior of $\omega^\Lambda_{z_0}(\mathbf{y})$ at large $|\mathbf{y}|$:

$$\omega^\Lambda_{z_0}(\mathbf{y})\simeq\frac{\Gamma(\frac{d+1}{2})}{\pi^{\frac{d+1}{2}}}\frac{z_0+\Lambda}{(z_0^2+|\mathbf{y}|^2)^{\frac{d+1}{2}}}+\cdots.$$

The accuracy of this relation can be improved by replacing z_0 by $z_0+\Lambda$ in the denominator. This is equivalent to replacing the exponential law in the average (68) by a Dirac distribution $\delta(z-\Lambda)$ centered at the mean traveled distance Λ:

$$\omega^\Lambda_{z_0}(\mathbf{y})\simeq\omega^0_{z_0+\Lambda}(\mathbf{y}). \tag{70}$$

Figure 3(b) shows that this approximation is more accurate for large $|\mathbf{y}|$ and small Λ, as expected.

Integrating Eq. (68) over $|\mathbf{y}|>R$, one gets

$$P^\Lambda_{z_0}(R)=\frac{2\Gamma(\frac{d+1}{2})}{\sqrt{\pi}\Gamma(\frac{d}{2})}\left[\int_0^{z_0/R}\frac{dx}{(x^2+1)^{\frac{d+1}{2}}}+\frac{1}{R}\int_0^\infty dz\frac{e^{-z/\Lambda}}{[1+(z+z_0)^2/R^2]^{\frac{d+1}{2}}}\right]. \tag{71}$$

In the limit $\Lambda\to 0$ (the harmonic measure), the second term vanishes, yielding

$$P^0_{z_0}(R)=\frac{2\Gamma(\frac{d+1}{2})}{\sqrt{\pi}\Gamma(\frac{d}{2})}\int_0^{z_0/R}\frac{dx}{(x^2+1)^{\frac{d+1}{2}}}. \tag{72}$$

For instance, one has

$$P^0_{z_0}(R)=\begin{cases}\frac{2}{\pi}\arctan(z_0/R) & (d=1),\\ \dfrac{z_0}{\sqrt{R^2+z_0^2}} & (d=2).\end{cases} \tag{73}$$

For higher dimensions, $P^0_{z_0}(R)$ can be found by differentiating these expressions:

$$P^0_{z_0}(R)=\frac{(-1)^n}{\Gamma(\frac{d}{2})}\lim_{x\to 1}\frac{\partial^n}{\partial x^n}\begin{cases}\frac{2\arctan(z_0/R/\sqrt{x})}{\sqrt{\pi}\sqrt{x}},\\ \frac{z_0/R}{x\sqrt{x+(z_0/R)^2}},\end{cases} \tag{74}$$

with the first line and $n=\frac{1}{2}(d-1)$ standing for odd dimensions d, while the second line and $n=\frac{1}{2}(d-2)$ for even dimensions.

Note that the approximation (70) for $\omega^\Lambda_{z_0}(\mathbf{y})$ yields a similar approximation for $P^\Lambda_{z_0}(R)$:

$$P^\Lambda_{z_0}(R)\approx P^0_{z_0+\Lambda}(R). \tag{75}$$

As illustrated in Fig. 4, this approximation is accurate for small Λ but becomes invalid for large Λ.

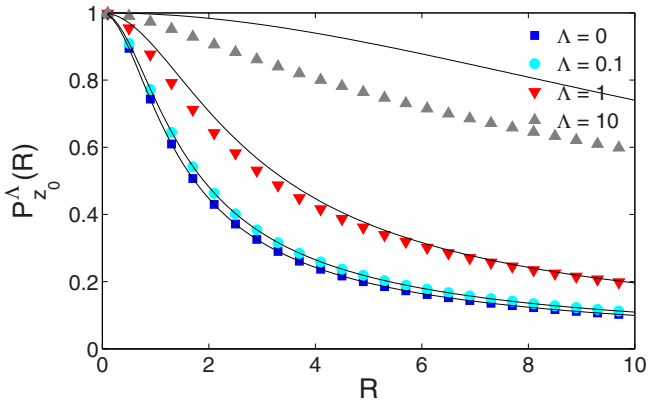

FIG. 4. (Color online) The probability $P^{\Lambda}_{z_0}(R)$ as a function of R for $d = 2$, $z_0 = 1$, and four values of Λ: 0, 0.1, 1, and 10. Symbols show the results of numerical integration in Eq. (67), while lines indicate the approximate relation (75), in which the exact relation (73) was used.

When $z_0 \to 0$, the first term in Eq. (71) vanishes, yielding

$$P^{\Lambda}_0(R) = \frac{2\Gamma\left(\frac{d+1}{2}\right)}{\sqrt{\pi}\,\Gamma\left(\frac{d}{2}\right)} \int_0^{\infty} dx \frac{e^{-xR/\Lambda}}{(1+x^2)^{\frac{d+1}{2}}}. \tag{76}$$

This expression illustrates that the length Λ determines the size of an interfacial region around the first hitting point on which the partially reflected Brownian motion is most likely to stop. In other words, multiple reflections after the first arrival onto the surface yield widening or spreading of the harmonic measure controlled by the length Λ: larger values of Λ correspond to more spread harmonic measures, and vice versa [52,59]. In particular, the median distance R_m [such that $P^{\Lambda}_0(R_m) = 1/2$] is proportional to Λ: $R_m \simeq 0.6232\Lambda$ for $d = 1$, $R_m \simeq 1.1702\Lambda$ for $d = 2$, etc.

It is worth noting that the spread harmonic measure density could also be obtained directly from Eq. (11), with the probability density $\rho^{\Lambda}_{z_0}(t)$ for the half-axis:

$$\rho^{\Lambda}_{z_0}(t) = \frac{De^{-z_0^2/(4Dt)}}{\Lambda^2}\left[\frac{\Lambda}{\sqrt{\pi Dt}} - \mathcal{K}\left(\frac{z_0}{\sqrt{4Dt}} + \frac{\sqrt{Dt}}{\Lambda}\right)\right], \tag{77}$$

where $\mathcal{K}(z) = \exp(z^2)\mathrm{erfc}(z)$ and $\mathrm{erfc}(z)$ is the complementary error function. In the limit $\Lambda \to 0$, one retrieves $\rho^0_{z_0}(t) = z_0 e^{-z_0^2/(4Dt)}/\sqrt{4\pi Dt^3}$. The above expression can be deduced from the survival probability on the positive semiaxis with a semipermeable boundary condition at the origin [see [61], Eq. (3.35)]:

$$S_{z_0}(t) = 1 - \mathrm{erfc}\left(\frac{z_0}{\sqrt{4Dt}}\right) + \exp\left(\frac{z_0}{\Lambda} + \frac{Dt}{\Lambda^2}\right)\mathrm{erfc}\left(\frac{z_0}{\sqrt{4Dt}} + \frac{\sqrt{Dt}}{\Lambda}\right). \tag{78}$$

We conclude this section by mentioning that the representation (68) of the spread harmonic measure density suggests a simple way to generate the stopping positions by generating the first *arrival* positions with random exponentially distributed height $z_0 + \zeta$. For this purpose, one can invert Eq. (73) [or, in general, Eq. (74)] to generate the distance R from the origin as

$$\begin{aligned} R &= (z_0 + \zeta)\mathrm{ctan}(\pi\mu/2) \quad (d = 1), \\ R &= (z_0 + \zeta)\sqrt{1/\mu^2 - 1} \quad (d = 2), \end{aligned} \tag{79}$$

where ζ obeys the exponential distribution with parameter Λ, and μ is an independent random variable uniformly distributed over the unit interval. The rotational symmetry allows one to transform the distance R to the position $\mathbf{y}$. For $d = 1$, one just needs to choose randomly the sign, i.e., $y = R\nu$, where ν is another random variable: $\nu = \pm 1$ with equal probabilities. For $d = 2$, one generates a point on the circle of radius R: $\mathbf{y} = (R\cos(2\pi\nu), R\sin(2\pi\nu))$, with ν being uniform over $[0,1]$. This scheme allows one to avoid the inversion of the integral relation (71).

III. DISCUSSION

While the harmonic measure characterizes the accessibility of different regions of a surface to Brownian motion, the spread harmonic measure describes the stopping positions of partially reflected Brownian motion by incorporating finite surface reactivity and the consequent multiple reflections. In addition, the spread harmonic measure density provides a solution of a general Laplacian boundary value problem: for a given $f(\mathbf{s})$, the function

$$u(\mathbf{x}_0) = \int_{\partial\Omega} d\mathbf{s}\, \omega^{\Lambda}_{\mathbf{x}_0}(\mathbf{s}) f(\mathbf{s}) \tag{80}$$

satisfies the Laplace equation $\Delta u(\mathbf{x}_0) = 0$ in Ω with the Robin boundary condition on $\partial\Omega$:

$$\left[u(\mathbf{x}_0) + \Lambda \frac{\partial}{\partial n} u(\mathbf{x}_0)\right]_{\mathbf{x}_0 = \mathbf{s}} = f(\mathbf{s}). \tag{81}$$

In fact, the density $\omega_{\mathbf{x}_0}(\mathbf{s})$ formally satisfies the Robin boundary condition

$$\left[\omega^{\Lambda}_{\mathbf{x}_0}(\mathbf{s}) + \Lambda \frac{\partial}{\partial n} \omega^{\Lambda}_{\mathbf{x}_0}(\mathbf{s})\right]_{\mathbf{x}_0 = \mathbf{s}_0} = \delta(\mathbf{s} - \mathbf{s}_0). \tag{82}$$

This relation suggests an important link to the Dirichlet-to-Neumann operator $\mathcal{M}$ [66]. For a function $f(\mathbf{s})$ on a smooth bounded boundary $\partial\Omega$, the operator $\mathcal{M}$ maps f to the normal derivative of a harmonic function u in Ω subject to the Dirichlet boundary condition $u = f$ on $\partial\Omega$. In other words, $\mathcal{M}f = (\frac{\partial u}{\partial n})_{|\partial\Omega}$, where u is the solution of the Laplace equation $\Delta u = 0$ subject to $u = f$ on $\partial\Omega$. Mathematically speaking, the operator $\mathcal{M}$ acts from the Sobolev space $H^1(\partial\Omega)$ to $L^2(\partial\Omega)$, and it is known to be a self-adjoint pseudodifferential operator of the first order, with a discrete positive spectrum $\{\mu_\alpha\}$ and smooth eigenfunctions forming a complete basis in $L^2(\partial\Omega)$ [66–71]. One can also define its resolvent operator $\mathcal{T}^{\Lambda} = [I + \Lambda\mathcal{M}]^{-1}$, called the *spreading operator*. This is an analytic operator function in the whole complex plane $\mathbb{C}$, except for a denumerable set of points, $\mathbb{C}\backslash\{-\mu_\alpha^{-1}\}$. In particular, $\mathcal{T}^{\Lambda}$ is well defined for any positive Λ [52]. Using the Dirichlet-to-Neumann operator, Eq. (82) can be written as

$$[\mathbf{I} + \Lambda\mathcal{M}]\omega^{\Lambda}_{\mathbf{s}_0}(\mathbf{s}) = \delta(\mathbf{s} - \mathbf{s}_0), \tag{83}$$

from which one concludes that $\mathcal{T}^{\Lambda}(\mathbf{s} - \mathbf{s}_0) = \omega^{\Lambda}_{\mathbf{s}_0}(\mathbf{s})$ is the kernel of the spreading operator $\mathcal{T}^{\Lambda}$. In particular, Eqs. (59)

and (68) with $z_0 = 0$ determine this kernel for a slab domain and for a half-space, respectively.

In analogy to the harmonic measure density [e.g., see Eq. (54)], the density $\omega^{\Lambda}_{\mathbf{x}_0}(\mathbf{s})$ can be expressed as

$$\omega^{\Lambda}_{\mathbf{x}_0}(\mathbf{s}) = -\left(\frac{\partial}{\partial n} G^{\Lambda}(\mathbf{x},\mathbf{x}_0)\right)_{\mathbf{x}=\mathbf{s}} = \frac{1}{\Lambda} G^{\Lambda}(\mathbf{s},\mathbf{x}_0), \tag{84}$$

where the Green function $G^{\Lambda}(\mathbf{x},\mathbf{x}_0)$ satisfies $\Delta_{\mathbf{x}} G^{\Lambda}(\mathbf{x},\mathbf{x}_0) = -\delta(\mathbf{x}-\mathbf{x}_0)$ in Ω, with the Robin boundary condition on $\partial\Omega$:

$$G^{\Lambda}(\mathbf{x},\mathbf{x}_0) + \Lambda \frac{\partial}{\partial n} G^{\Lambda}(\mathbf{x},\mathbf{x}_0) = 0. \tag{85}$$

Note that the Green function is directly related to the propagator:

$$G^{\Lambda}(\mathbf{x},\mathbf{x}_0) = D \int_0^{\infty} dt\, G_t(\mathbf{x},\mathbf{x}_0) \tag{86}$$

(this relation is not applicable for the Neumann case when $\Lambda = \infty$). Although the spread harmonic measure density ignores the temporal aspects of diffusion, it can be computed by using either the propagator or the Green function. In practice, the former approach is often simpler. For instance, the propagator on the semiaxis is known as [62,72]

$$G^{\perp}_t(z,z_0) = \frac{\exp\left(-\frac{(z-z_0)^2}{4Dt}\right) + \exp\left(-\frac{(z+z_0)^2}{4Dt}\right)}{\sqrt{4\pi\, Dt}} - \frac{1}{\Lambda} \exp\left(\frac{2}{\Lambda}(z+z_0+2\kappa t)\right) \times \operatorname{erfc}\left(\frac{z+z_0+4\kappa t}{\sqrt{4Dt}}\right), \tag{87}$$

where $\kappa = D/\Lambda$ is the surface reactivity. Multiplying this expression by the lateral propagator (12) and integrating by t from 0 to ∞, one gets the corresponding Green function

$$G^{\Lambda}(\mathbf{x},\mathbf{x}_0) = g(\mathbf{x},\mathbf{x}_0) + g(\mathbf{x},\mathbf{x}'_0) - \frac{D}{\Lambda} \int_0^{\infty} dt \frac{\exp\left(-\frac{|\mathbf{y}-\mathbf{y}_0|^2}{4Dt}\right)}{(4\pi\, Dt)^{d/2}} \times \exp\left(\frac{2}{\Lambda}(z+z_0+2\kappa t)\right) \operatorname{erfc}\left(\frac{z+z_0+4\kappa t}{\sqrt{4Dt}}\right), \tag{88}$$

where $g(\mathbf{x},\mathbf{x}_0)$ is given by Eq. (56), and $\mathbf{x}'_0$ is the mirror reflection of $\mathbf{x}_0$ with respect to the hyperplane $z = 0$. Rearranging terms and writing the last integral through the density $\rho^{\Lambda}_{z_0}(t)$ from Eq. (77), one can recognize in the last term the general form (11) for the spread harmonic measure density, from which

$$G^{\Lambda}(\mathbf{x},\mathbf{x}_0) = g(\mathbf{x},\mathbf{x}_0) - g(\mathbf{x},\mathbf{x}'_0) + \Lambda \omega^{\Lambda}_{z+z_0}(\mathbf{y}-\mathbf{y}_0). \tag{89}$$

In turn, the density $\omega^{\Lambda}_{z+z_0}(\mathbf{y}-\mathbf{y}_0)$ can be represented according to Eq. (68). Setting $z = 0$, one retrieves Eq. (84).

A. Diffusion in cylindrical domains

Although this paper was focused on the spread harmonic measure on slab domains, there are other practically relevant examples. For instance, for an infinite cylinder $\Omega = \mathbb{R} \times \Omega_{\perp}$ of an arbitrary *bounded* cross section $\Omega_{\perp} \subset \mathbb{R}^{d_{\perp}}$, Eq. (20) yields

$$\omega^{\Lambda}_{\mathbf{z}_0}(y) = \frac{1}{2} \sum_{m=1}^{\infty} \frac{c_m(\mathbf{z}_0)}{\sqrt{\lambda_m}} \exp(-\sqrt{\lambda_m}|y|). \tag{90}$$

Among all bounded domains of the same volume, the ball minimizes the first eigenvalue λ_1. This statement is known as the Rayleigh-Faber-Krahn isoperimetric inequality for the Dirichlet boundary condition ($\Lambda = 0$), and it was extended by Daners for the Robin boundary condition ($\Lambda > 0$) [73,74] (see [75,76] for reviews). As a consequence, the slowest decay rate $\sqrt{\lambda_1}$ is achieved for a ball in $\mathbb{R}^{d_{\perp}}$. In particular, among all cylinders of cross-sectional area πL^2 embedded into the three-dimensional space (with $d_{\perp} = 2$), the circular cylinder of radius L provides the slowest lateral decay, with $\lambda_1 = \alpha_1^2/L^2$, where $\alpha_1 \approx 2.4048\ldots$ is the first zero of the Bessel function $J_0(z)$.

When the cross section $\Omega_{\perp}$ of a cylindrical domain is not bounded, one needs first to solve Eqs. (8) and (9) for the transverse diffusion propagator in order to get the probability density $\rho_{\mathbf{z}_0}(t)$ of the stopping time. This problem can be solved analytically for rotation-invariant domains [26]. For instance, if $\Omega_{\perp} = \{\mathbf{z} \in \mathbb{R}^2 : |\mathbf{z}| > L\}$ is the exterior of the disk of radius L, the first-passage time density can be written through the inverse Laplace transform (denoted as $\mathcal{L}_t^{-1}$) [77]

$$\rho^0_{\mathbf{z}_0}(t) = \mathcal{L}_t^{-1}\left\{\frac{K_0(|\mathbf{z}_0|\sqrt{s/D})}{K_0(L\sqrt{s/D})}\right\}. \tag{91}$$

Since the modified Bessel function $K_0(z)$ is positive in the whole complex plane (see [78], p. 511), the residue theorem is not applicable (in contrast to the usual case), and one needs to perform the Laplace inversion numerically. At long times, the probability density exhibits very slow decay [79],

$$\rho^0_{\mathbf{z}_0}(t) \simeq \frac{2(|\mathbf{z}_0|/L - 1)}{t \ln^2(2Dt/L^2)} \quad (t \gg L^2/D), \tag{92}$$

i.e., very long transverse excursions remain probable. An extension of Eq. (91) to a partially reactive boundary is straightforward:

$$\rho^{\Lambda}_{\mathbf{z}_0}(t) = \mathcal{L}_t^{-1}\left\{\frac{K_0(|\mathbf{z}_0|\sqrt{s/D})}{K_0(L\sqrt{s/D}) + \Lambda\sqrt{s/D} K_1(L\sqrt{s/D})}\right\}. \tag{93}$$

Although the explicit representation of $\rho^{\Lambda}_{\mathbf{z}_0}(t)$ is not available, the probability density of relocations along the cylinder (i.e., precisely the spread harmonic measure density along the cylinder axis) can be found by using Eq. (14):

$$\omega^{\Lambda}_{\mathbf{z}_0}(y) = \frac{1}{L} \int_0^{\infty} \frac{d\alpha}{\pi} \frac{\cos(\alpha y/L) K_0(\alpha|\mathbf{z}_0|/L)}{K_0(\alpha) + \alpha h K_1(\alpha)} \tag{94}$$

(this expression was first derived in [15]). Long transverse excursions imply long lateral relocations:

$$\omega^{\Lambda}_{\mathbf{z}_0}(y) \simeq \frac{\Lambda/L + \ln(|\mathbf{z}_0|/L)}{2|y| \ln^2(|y|/L)} \quad (|y| \gg L). \tag{95}$$

This asymptotic behavior is drastically different from the exponentially fast decay for diffusion inside the cylinder. The statistics of relocations by bulk diffusion can be used to study intermittent diffusion in which bulk and surface diffusion alternate (see [80–83] and references therein).

B. Diffusion near a reflecting boundary

Diffusion in a thin layer near a reflecting boundary is often substituted by surface diffusion. In this model, a particle diffuses on the surface until a random stopping time, after which it is ejected above the surface to a distance a. The desorption events are typically modeled by an exponential law with a prescribed desorption rate λ, i.e., with $\rho(t) = \lambda e^{-\lambda t}$ [80,81]. For a flat surface, the probability density of desorption positions follows from Eq. (11):

$$\hat{\omega}_a(\mathbf{y}) = \frac{(|\mathbf{y}|/a)^{1-\frac{d}{2}}}{a^d(2\pi)^{\frac{d}{2}}}(\lambda a^2/D)^{\frac{d+2}{4}} K_{\frac{d}{2}-1}(|\mathbf{y}|\sqrt{\lambda/D}). \quad (96)$$

As expected, this expression is very similar to Eq. (20), in which only one exponential term is kept and $D\lambda_1/a^2$ is replaced by λ. In other words, setting $\lambda = D\lambda_1/a^2$, one achieves the same asymptotic behavior at large distances for both densities $\hat{\omega}_a(\mathbf{y})$ and $\omega^0_{a,a}(\mathbf{y})$. This is not surprising because the first exit time density $\rho^0_{z_0,a}(t)$ resembles an exponential law at long times. If the exponential law for desorption events was replaced by $\rho^0_{z_0,a}(t)$, both models would yield exactly the same densities of desorption positions. Note that the probability density $\omega^0_{a,a}(\mathbf{y})$ of exit points from a layer of width a above the reflecting flat boundary can be obtained by setting $h = 0$ and $h_1 = \infty$ (Neumann boundary condition).

C. Anomalous diffusion

To incorporate long-time trapping events and the consequent subdiffusive behavior in complex systems, normal diffusion is often replaced by continuous-time random walks (CTRWs) [84–86]. This model has been thoroughly studied; in particular, the survival probability and the effect of a partially reactive boundary on the probability density of the stopping times were investigated [87–89]. In mathematical terms, a CTRW can be described by an appropriate time subordination of Brownian motion or, equivalently, by replacing a diffusion equation by a fractional diffusion equation. As a consequence, both lateral and transverse propagators, as well as the probability density of the stopping time, will be changed [84,88]:

$$\mathcal{L}_s\left\{\rho^{\Lambda}_{z_0}(t)\right\} = \frac{e^{-z_0\sqrt{s^\alpha/D_\alpha}}}{1+\Lambda\sqrt{s^\alpha/D_\alpha}} \quad (97)$$

and

$$\mathcal{L}_s\{G^{||}_t(\mathbf{y}_0,\mathbf{y})\} = \frac{s^{-1}\left(s^\alpha/D_\alpha\right)^{\frac{d}{2}}}{(2\pi)^{\frac{d}{2}}} \frac{K_{\frac{d}{2}-1}\left(|\mathbf{y}-\mathbf{y}_0|\sqrt{\frac{s^\alpha}{D_\alpha}}\right)}{\left(|\mathbf{y}-\mathbf{y}_0|\sqrt{\frac{s^\alpha}{D_\alpha}}\right)^{\frac{d}{2}-1}}, \quad (98)$$

where D_α is the generalized diffusion coefficient, and $0 < \alpha \leqslant 1$ is the scaling exponent ($\alpha = 1$ corresponds to normal diffusion). A physical interpretation of the length Λ for a CTRW is provided in [90]. In general, both α and D_α can be different for lateral and transverse motion.

When only the transverse motion is anomalous, Eq. (14) can be applied to compute the spread harmonic measure density in the half-space for a probability density of the stopping time given in the Laplace space. Substituting Eq. (97), one gets for the transverse CTRW:

$$\omega^{\Lambda}_{z_0}(\mathbf{y}) = \frac{|\mathbf{y}|^{1-\frac{d}{2}}}{(2\pi)^{\frac{d}{2}}}\int_0^\infty dk\, k^{\frac{d}{2}} J_{\frac{d}{2}-1}(|\mathbf{y}|k)\frac{e^{-z_0\eta k^\alpha}}{1+\Lambda\eta k^\alpha}, \quad (99)$$

where $\eta = \sqrt{D^\alpha_{||}/D_\alpha}$ and D_α characterizes anomalous diffusion in the transverse direction. For $\alpha = 1$, one retrieves Eq. (66).

When both lateral and transverse motions are anomalous, the above trick does not work, and a numerical inversion of the Laplace transforms in Eqs. (97) and (98) is needed to compute the spread harmonic measure by Eq. (11), which incorporates $\rho^{\Lambda}_{z_0}(t)$ and $G^{||}_t(\mathbf{y}_0,\mathbf{y})$ in the time domain. Even when lateral and transverse CTRWs are characterized by the same α and D_α, the computation is difficult. It is worth stressing that the process with two independent CTRWs for lateral and transverse directions is not equivalent to a single CTRW with independent displacements in these directions. In fact, every CTRW is characterized by random displacements and random waiting times. In the former case of two CTRWs, lateral and transverse displacements are independent and occur at different waiting times (independent from each other). In turn, for a single CTRW, lateral and transverse displacements are still independent, but they occur at the same moments. This subtle difference changes the spread harmonic measure. For a single CTRW, the probability distribution of the stopping points is still described by the spread harmonic measure density derived for Brownian motion because long trapping events do not affect spatial displacements. Roughly speaking, the spread harmonic measure ignores the fact that the arrival to the stopping position by a CTRW may take much longer than by Brownian motion. Figuratively speaking, Brownian motion and CTRW generate the same spatial path but move along it at different paces.

To illustrate the difference between these two situations, we consider an example of CTRW with $\alpha = 2/3$, $d = 1$, and $\Lambda = 0$, for which the inverse Laplace transforms in Eqs. (97) and (98) can be found explicitly:

$$\rho^0_{z_0}(t) = \frac{(z_0/\sqrt{D_\alpha})^{\frac{3}{2}}}{3\pi t^{\frac{3}{2}}} K_{\frac{1}{3}}\left[2\left(\frac{z_0/3}{\sqrt{D_\alpha t^{2/3}}}\right)^{\frac{3}{2}}\right],$$
$$G^{||}_t(\mathbf{y}_0,\mathbf{y}) = \frac{(|\mathbf{y}-\mathbf{y}_0|/\sqrt{D_\alpha})^{\frac{1}{2}}}{2\pi\sqrt{D_\alpha}\sqrt{t}} K_{\frac{1}{3}}\left[2\left(\frac{|\mathbf{y}-\mathbf{y}_0|/3}{\sqrt{D_\alpha t^{2/3}}}\right)^{\frac{3}{2}}\right]. \quad (100)$$

Substituting these expressions into Eq. (11) yields, after simplifications, the harmonic measure density

$$\omega^0_{z_0}(y) = \frac{3\sqrt{3}}{4\pi}\frac{z_0}{z_0^2 + z_0|y| + y^2}. \quad (101)$$

This expression differs from the Cauchy distribution (52) for Brownian motion. We conclude that the distribution of first arrivals of CTRW onto a flat surface is affected by distinct waiting times for lateral and transverse motions. The same conclusion holds for the spread harmonic measure.

D. Several extensions

In conclusion, we mention several extensions of the above results.

(i) The convolution (11) includes all stopping times from 0 to infinity. For some applications, it may be convenient to consider a restricted range $[t_{\min},t_{\max}]$ of stopping times at which the distribution of stopping points is determined (e.g., $t_{\min}$ can mimic a delay between the beginning of experiment and switching on a camera, while $t_{\max}$ can be the duration of experiment). However, the related integrals have to be computed numerically.

(ii) Throughout the paper, we considered unrestricted lateral motion in $\Omega_{||} = \mathbb{R}^d$. Using the method of images, the above analysis can be extended to a half-space $\mathbb{R}^{d-1} \times \mathbb{R}_+$ or a hyperoctant $\mathbb{R}^d_+$ (or any Cartesian product of $\mathbb{R}$ and $\mathbb{R}_+$) with an absorbing surface [e.g., the diffusion propagator on the positive semiaxis reads $G_t(x_0,x) - G_t(-x_0,x)$, where $G_t(x_0,x)$ is given by Eq. (12)]. For instance, one can easily compute the spread harmonic measure on a half-cylinder.

(iii) In addition to diffusion inside and outside a circular cylinder, one can compute the spread harmonic measure for diffusion between two coaxial cylinders. Due to the rotational symmetry, the eigenvalues and eigenfunctions of the Laplace operator are known explicitly [26,61,62,76]. The effect of curvature of the cylindrical surface can be investigated.

(iv) For both cylinders and slab domains, one can include a drift or an external potential in the transverse direction. For instance, the probability density of the first-passage time at the origin of the semiaxis for a drifted particle with speed v is [26]

$$\rho^0_{z_0}(t) = \frac{z_0}{\sqrt{4\pi Dt^3}} \exp\left(-\frac{(z_0+vt)^2}{4Dt}\right). \qquad (102)$$

Integrating this density with the Gaussian propagator (12) for the lateral motion yields the harmonic measure density in the drifted case. For a partially reflecting boundary, one deduces

$$\rho^\Lambda_{z_0}(t) = \frac{De^{-(z_0+vt)^2/(4Dt)}}{\Lambda^2} \times \left\{\frac{\Lambda}{\sqrt{\pi Dt}} - \mathcal{K}\left[\frac{z_0}{\sqrt{4Dt}} + \frac{\sqrt{Dt}}{\Lambda}\left(1 - \frac{v\Lambda}{2D}\right)\right]\right\}, \qquad (103)$$

in analogy with Eq. (77). Another explicit formula for the first-passage time density is known for the harmonically trapped particles on the semiaxis [91],

$$\rho^0_{z_0}(t) = \frac{z_0[\sinh(t/\tau)]^{-\frac{3}{2}}}{\sqrt{4\pi D\tau^3}} \exp\left(-\frac{z_0^2}{4D\tau}\frac{e^{-t/\tau}}{\sinh(t/\tau)} + \frac{t}{2\tau}\right), \qquad (104)$$

where $\tau = k_BT/(kD)$ is the trapping time (expressed through the harmonic potential strength k, the Boltzmann constant k_B, and the absolute temperature T). The exit time problem of a harmonically trapped particle from an interval was reviewed in [92]. In cases when only the Laplace transform of $\rho_{z_0}(t)$ is available, Eq. (14) can be used to compute the spread harmonic measure density.

(v) According to Eq. (43), the harmonic measure density in a half-space $\mathbb{R}^d \times \mathbb{R}_+$ decays as a power law: $\omega^0_{z_0}(\mathbf{y}) \propto |\mathbf{y}|^{-d-1}$ at large $|\mathbf{y}|$. As a consequence, the probability density of excursion distances $r = |\mathbf{y}|$ (once averaged over the angular part) decays as $r^{-\beta}$, with the scaling exponent $\beta = 2$. The probability density of the stopping times also exhibits a power-law decay, $\rho^0_{z_0}(t) \propto t^{-\alpha}$, with $\alpha = 3/2$. The statistics of the first-passage times and the excursion distances over *irregular* boundaries were shown to decay as power laws as well, with $\alpha = (d_f - d_e + 4)/2$ and $\beta = d_f - d_e + 3$, where d_f is the fractal dimension of the boundary and d_e is the embedding dimension (here, $d_e = d + 1$) [93]. For a smooth boundary, $d_f = d_e - 1$, from which $\alpha = 3/2$ and $\beta = 2$ are retrieved. An extension of the above scaling relations to the spread harmonic measure on irregular boundaries presents an interesting perspective. Some multifractal properties of the spread harmonic measure distribution on fractal boundaries were already studied [59].

IV. CONCLUSION

In this paper, we obtained various analytical representations of the spread harmonic measure density in Euclidean domains, in which Brownian motion can be split into independent lateral and transverse displacements. This measure characterizes the spatial distribution of the stopping position of the lateral motion under the stopping criterion set by the transverse motion. For slab domains $\mathbb{R}^d \times [0,L]$, we derived both the series and integral representations of the spread harmonic measure density $\omega^\Lambda_{z_0,L}(\mathbf{y})$ and showed its exponential decay at large distances $|\mathbf{y}|$. In turn, long-time excursions in a half-space ($L = \infty$) were shown to lead to a slower, power-law decay. In this case, we argued that the spread harmonic measure could be interpreted as the average of the harmonic measure over exponentially distributed starting points. The mean traveled distance Λ of the transverse motion in the vicinity of the surface was related to both the macroscopic and microscopic parameters of Laplacian transfer. It was shown to determine the size of the interfacial region (around the first arrival point) on which reaction mainly occurs, and to control the spreading effect due to multiple reflections on the surface. We discussed the relation between the spread harmonic measure density, the Dirichlet-to-Neumann operator and the Green function, the modeling of diffusion near a reflecting boundary by surface diffusion, as well as several extensions, such as diffusion in cylindrical domains, limited duration of experiment, and anomalous diffusion.

ACKNOWLEDGMENTS

The author thanks S. Smirnov for stimulating this work, and acknowledges partial support under Grant No. ANR-13-JSV5-0006-01 of the French National Research Agency.

APPENDIX: CONVERGENCE AND PRACTICAL IMPLEMENTATION

We briefly discuss the convergence of the main results and their practical implementation. At the same time, rigorous mathematical statements and proofs, as well as challenges related to irregular domains, remain beyond the scope of the paper.

For any bounded transverse domain $\Omega_\perp$, the series (20) and similar expansions converge exponentially for any $|\mathbf{y}| > 0$. In fact, the asymptotic growth of the Laplacian eigenvalues ($\lambda_m \to \infty$ as $m \to \infty$) implies that $z = \eta\sqrt{\lambda_m}|\mathbf{y}|$ becomes large enough so that the modified Bessel function $K_{\frac{d}{2}-1}(z)$ decays exponentially according to Eq. (25). This ensures the converges of the series (20) given that the coefficients $c_m(\mathbf{z}_0)$ exhibit a power-law dependence on m (or λ_m). In practice, if $|\mathbf{y}|$ is too small, a very large number of terms is needed to get accurate results that would make the computation inefficient. In this case, integral representations are more convenient.

Note that the limiting value $|\mathbf{y}| = 0$ would require a more subtle analysis of the series (20). If one needs to compute $\omega^\Lambda_{\mathbf{z}_0}(0)$, it is easier to substitute $G^{||}_t(\mathbf{y}_0,\mathbf{y})$ from Eq. (12) at $\mathbf{y}_0 = \mathbf{y} = \mathbf{0}$ into Eq. (11) to get

$$\omega^\Lambda_{\mathbf{z}_0}(0) = \int_0^\infty dt(4\pi D_{||}t)^{-d/2}\rho_{\mathbf{z}_0}(t) = \frac{\langle\tau^{-d/2}\rangle_{\mathbf{z}_0}}{(4\pi D_{||})^{d/2}}. \quad \text{(A1)}$$

In other words, $\omega^\Lambda_{\mathbf{z}_0}(0)$ is proportional to the moment of order $-d/2$ of the stopping time τ. This moment is finite for any starting point $\mathbf{z}_0$ *inside* the transverse domain $\Omega_\perp$ (i.e., not on the boundary $\partial\Omega_\perp$). In fact, the above integral converges at large times since the probability density $\rho_{\mathbf{z}_0}(t)$ is normalized, and at short times due to its very rapid decay:

$$\rho_{\mathbf{z}_0}(t) \propto \exp\left(-\frac{|\mathbf{z}_0 - \partial\Omega_\perp|^2}{4D_\perp t}\right) \quad (t \to 0) \quad \text{(A2)}$$

(here $|\mathbf{z}_0 - \partial\Omega_\perp|$ is the distance from $\mathbf{z}_0$ to the boundary $\partial\Omega_\perp$ or its "target region" S).

All integral representations of $\omega^\Lambda_{\mathbf{z}_0}(\mathbf{y})$ are equally well-converging. For instance, the integrand of the second relation in Eq. (14) behaves like k^{d-1} as $k \to 0$ [given that the Laplace transform $\mathcal{L}_{D_{||}k^2}\{\rho_{\mathbf{z}_0}(t)\}$ approaches 1 due to the normalization of $\rho_{\mathbf{z}_0}(t)$], and decays exponentially as $k \to \infty$ [that follows from the asymptotic behavior (A2)]. This exponential decay is clearly seen, for instance, in Eqs. (47), (48), (45), and (61). In practice, the upper limit of the integrals is truncated by a large enough number to ensure that the remaining part is negligible. For a prescribed precision ϵ, the integral in Eq. (61) (or similar) can be truncated to $\alpha_{\max}$ such that $\frac{\sinh\alpha(1-z_0/L)}{\sinh\alpha} \simeq e^{-\alpha z_0/L} < \epsilon$ for $\alpha \geqslant \alpha_{\max}$. The finite integral from 0 to $\alpha_{\max}$ can then be computed by Gauss quadratures or other numerical methods. When $|\mathbf{y}|$ is very large, the Bessel function $J_{\frac{d}{2}-1}(\alpha|\mathbf{y}|/L)$ rapidly oscillates that may require very fine discretizations and thus slow down computations. In this case, the series expansions are more suitable. Combining these complementary representations is an efficient way to compute the probability density $\omega^\Lambda_{\mathbf{z}_0}(\mathbf{y})$.

When the starting point $\mathbf{z}_0$ belongs to the boundary $\partial\Omega_\perp$, some of the above arguments fail. For instance, the harmonic measure density degenerates to the Dirac distribution $\delta(\mathbf{y})$, and the convergence analysis of series and integral representations should be refined. While this point is less relevant for the spread harmonic measure density (which does not degenerate to a singular distribution), the discussion of convergence issues in this case is beyond the scope of the paper.

[1] F. C. Collins and G. E. Kimball, Diffusion-controlled reaction rates, J. Colloid Sci. **4**, 425 (1949).

[2] G. Wilemski and M. Fixman, General theory of diffusion-controlled reactions, J. Chem. Phys. **58**, 4009 (1973).

[3] H. Sano and M. Tachiya, Partially diffusion-controlled recombination, J. Chem. Phys. **71**, 1276 (1979).

[4] A. Szabo, K. Schulten, and Z. Schulten, First passage time approach to diffusion controlled reactions, J. Chem. Phys. **72**, 4350 (1980).

[5] M. Tachiya, Theory of diffusion-controlled reactions: Formulation of the bulk reaction rate in terms of the pair probability, Radiat. Phys. Chem. **21**, 167 (1983).

[6] G. H. Weiss, Overview of theoretical models for reaction rates, J. Stat. Phys. **42**, 3 (1986).

[7] A. V. Barzykin and M. Tachiya, Diffusion-influenced reaction kinetics on fractal structures, J. Chem. Phys. **99**, 9591 (1993).

[8] M.-O. Coppens, The effect of fractal surface roughness on diffusion and reaction in porous catalysts: From fundamentals to practical applications, Catal. Today **53**, 225 (1999).

[9] O. Bénichou, M. Coppey, M. Moreau, and G. Oshanin, Kinetics of diffusion-limited catalytically activated reactions: An extension of the Wilemski-Fixman approach, J. Chem. Phys. **123**, 194506 (2005).

[10] J. M. Schurr, The role of diffusion in enzyme kinetic, Biophys. J. **10**, 717 (1970).

[11] D. Shoup and A. Szabo, Role of diffusion in ligand binding to macromolecules and cell-bound receptors, Biophys. J. **40**, 33 (1982).

[12] S. F. Burlatsky and G. Oshanin, Diffusion-controlled reactions with polymers, Phys. Lett. A **145**, 61 (1990).

[13] D. Holcman and Z. Schuss, Stochastic chemical reactions in microdomains, J. Chem. Phys. **122**, 114710 (2005).

[14] P. C. Bressloff, B. A. Earnshaw, and M. J. Ward, Diffusion of protein receptors on a cylindrical dendritic membrane with partially absorbing traps, SIAM J. Appl. Math. **68**, 1223 (2008).

[15] C. Loverdo, O. Bénichou, R. Voituriez, A. Biebricher, I. Bonnet, and P. Desbiolles, Quantifying hopping and jumping in facilitated diffusion of DNA-binding proteins, Phys. Rev. Lett. **102**, 188101 (2009).

[16] P. C. Bressloff and J. Newby, Stochastic models of intracellular transport, Rev. Mod. Phys. **85**, 135 (2013).

[17] O. Bénichou and R. Voituriez, From first-passage times of random walks in confinement to geometry-controlled kinetics, Phys. Rep. **539**, 225 (2014).

[18] K. R. Brownstein and C. E. Tarr, Importance of classical diffusion in NMR studies of water in biological cells, Phys. Rev. A **19**, 2446 (1979).

[19] A. Coy and P. Callaghan, Pulsed gradient spin echo nuclear magnetic resonance for molecules diffusing between partially reflecting rectangular barriers, J. Chem. Phys. **101**, 4599 (1994).

[20] P. N. Sen, L. M. Schwartz, P. P. Mitra, and B. I. Halperin, Surface relaxation and the long-time diffusion coefficient in porous media: Periodic geometries, Phys. Rev. B **49**, 215 (1994).
[21] P. W. Kuchel, A. J. Lennon, and C. Durrant, Analytical solutions and simulations for spin-echo measurements of diffusion of spins in a sphere with surface and bulk relaxation, J. Magn. Reson. B **112**, 1 (1996).
[22] S. Godefroy, J.-P. Korb, M. Fleury, and R. G. Bryant, Surface nuclear magnetic relaxation and dynamics of water and oil in macroporous media, Phys. Rev. E **64**, 021605 (2001).
[23] A. Valfouskaya, P. M. Adler, J.-F. Thovert, and M. Fleury, Nuclear magnetic resonance diffusion with surface relaxation in porous media, J. Coll. Int. Sci. **295**, 188 (2006).
[24] D. S. Grebenkov, NMR survey of reflected Brownian motion, Rev. Mod. Phys. **79**, 1077 (2007).
[25] S. Ryu and D. L. Johnson, Aspects of diffusive-relaxation dynamics with a nonuniform, partially absorbing boundary in general porous media, Phys. Rev. Lett. **103**, 118701 (2009).
[26] S. Redner, *A Guide to First Passage Processes* (Cambridge University Press, Cambridge, 2001).
[27] *First-Passage Phenomena and Their Applications*, edited by R. Metzler, G. Oshanin, S. Redner (World Scientific, Singapore, 2014).
[28] Z. Schuss, *Brownian Dynamics at Boundaries and Interfaces: In Physics, Chemistry, and Biology* (Springer, New York, 2013).
[29] R. de Levie, The influence of surface roughness of solid electrodes on electrochemical measurements, Electrochim. Acta **10**, 113 (1965).
[30] L. Nyikos and T. Pajkossy, Fractal dimension and fractional power frequency-dependent impedance of blocking electrodes, Electrochim. Acta **30**, 1533 (1985).
[31] T. Pajkossy, Electrochemistry at fractal surfaces, J. Electroanal. Chem. **300**, 1 (1991).
[32] P. Meakin and B. Sapoval, Random-walk simulation of the response of irregular or fractal interfaces or membranes, Phys. Rev. A **43**, 2993 (1991).
[33] T. C. Halsey and M. Leibig, Random walks and the double layer impedance, Europhys. Lett. **14**, 815 (1991).
[34] T. C. Halsey and M. Leibig, The double layer impedance at a rough surface. Theoretical results, Ann. Phys. (N.Y.) **219**, 109 (1992).
[35] B. Sapoval, General formulation of Laplacian transfer across irregular surfaces, Phys. Rev. Lett. **73**, 3314 (1994).
[36] M. Filoche and B. Sapoval, Can one hear the shape of an electrode? II. Theoretical study of the Laplacian transfer, Eur. Phys. J. B **9**, 755 (1999).
[37] D. S. Grebenkov, M. Filoche, and B. Sapoval, Mathematical basis for a general theory of Laplacian transport towards irregular interfaces, Phys. Rev. E **73**, 021103 (2006).
[38] J. B. Garnett and D. E. Marshall, *Harmonic Measure* (Cambridge University Press, Cambridge, 2005).
[39] J. B. Garnett, *Applications of Harmonic Measure* (Wiley, New York, 1986).
[40] P. Meakin, *Fractals, Scaling and Growth far from Equilibrium* (Cambridge University Press, Cambridge, England, 1998).
[41] T. Vicsek, *Fractal Growth Phenomena*, 2nd ed. (World Scientific, Singapore, 1992).
[42] B. Sapoval, Transport Across Irregular Interfaces: Fractal Electrodes, Membranes and Catalysts, in *Fractals and Disordered Systems*, edited by A. Bunde and S. Havlin (Springer, Berlin, 1996).
[43] J. D. Jackson, *Classical Electrodynamics*, 3rd ed. (Wiley, New York, 1999).
[44] N. G. Makarov, On the distortion of boundary sets under conformal mappings, Proc. London Math. Soc. **51**, 369 (1985).
[45] B. B. Mandelbrot and C. J. G. Evertsz, The potential distribution around growing fractal clusters, Nature (London) **348**, 143 (1990).
[46] C. J. G. Evertsz and B. B. Mandelbrot, Harmonic measure around a linearly self-similar tree, J. Phys. A **25**, 1781 (1992).
[47] N. G. Makarov, Fine structure of harmonic measure, St. Petersburg Math. J. **10**, 217 (1999).
[48] B. Duplantier, Harmonic measure exponents for two-dimensional percolation, Phys. Rev. Lett. **82**, 3940 (1999).
[49] D. S. Grebenkov, What makes a boundary less accessible, Phys. Rev. Lett. **95**, 200602 (2005).
[50] D. S. Grebenkov, A. A. Lebedev, M. Filoche, and B. Sapoval, Multifractal properties of the harmonic measure on Koch boundaries in two and three dimensions, Phys. Rev. E **71**, 056121 (2005).
[51] D. A. Adams, L. M. Sander, E. Somfai, and R. M. Ziff, The harmonic measure of diffusion-limited aggregates including rare events, Eur. Phys. Lett. **87**, 20001 (2009).
[52] D. S. Grebenkov, Partially Reflected Brownian Motion: A Stochastic Approach to Transport Phenomena, in *Focus on Probability Theory*, edited by L. R. Velle (Nova Science, Hauppauge, NY, 2006), p. 135.
[53] D. S. Grebenkov, Residence times and other functionals of reflected Brownian motion, Phys. Rev. E **76**, 041139 (2007).
[54] A. Singer, Z. Schuss, A. Osipov, and D. Holcman, Partially reflected diffusion, SIAM J. Appl. Math. **68**, 844 (2008).
[55] F. Rojo, H. S. Wio, and C. E. Budde, Narrow-escape-time problem: The imperfect trapping case, Phys. Rev. E **86**, 031105 (2012).
[56] K. Itô and H. P. McKean, *Diffusion Processes and Their Sample Paths* (Springer-Verlag, Berlin, 1965).
[57] P. Lévy, *Processus Stochastiques et Mouvement Brownien* (Gauthier-Villard, Paris, 1965).
[58] B. Sapoval, J. S. Andrade, A. Baldassarri, A. Desolneux, F. Devreux, M. Filoche, D. S. Grebenkov, and S. Russ, New simple properties of a few irregular systems, Physica A **357**, 1 (2005).
[59] D. S. Grebenkov, Scaling properties of the spread harmonic measures, Fractals **14**, 231 (2006).
[60] D. S. Grebenkov, M. Filoche, and B. Sapoval, Spectral properties of the Brownian self-transport operator, Eur. Phys. J. B **36**, 221 (2003).
[61] J. Crank, *The Mathematics of Diffusion* (Oxford University Press, Oxford, 1956).
[62] H. S. Carslaw and J. C. Jaeger, *Conduction of Heat in Solids*, 2nd ed. (Oxford University Press, Oxford, 1959).
[63] B. D. Hughes, *Random Walks and Random Environments* (Clarendon, Oxford, 1995).
[64] G. F. Roach, *Green's Functions*, 2nd ed. (Cambridge University Press, Cambridge, 1982).
[65] D. G. Duffy, *Green's Functions with Applications*, 2nd ed. (Chapman & Hall/CRC Press, Boca Raton, 2015).
[66] M. S. Agranovich, Elliptic Boundary Problems, in *Partial Differential Equations IX*, edited by M. S. Agranovich, Yu.

V. Egorov, and M. S. Shubin, Encyclopaedia of Mathematical Sciences (Springer, Berlin, 1997), Vol. 79.

[67] M. S. Birman and M. Z. Solomyak, *Spectral Theory of Self-Adjoint Operators in Hilbert Space* (Reidel, Dordrecht, 1987).

[68] L. Hörmander, *The Analysis of Linear Partial Differential Operators* (Springer, Berlin, 1983).

[69] Yu. Egorov, *Pseudo-differential Operators, Singularities, Applications* (Birkhauser, Basel, 1997).

[70] N. Jacob, *Pseudo-differential Operators and Markov Processes* (Akademie-Verlag, Berlin, 1996).

[71] M. E. Taylor, *Pseudodifferential Operators* (Princeton University Press, Princeton, 1981).

[72] G. H. Bryan, Note on a problem in the linear conduction of heat, Proc. Camb. Phil. Soc. **7**, 246 (1891).

[73] D. Daners, A Faber-Krahn inequality for Robin problems in any space dimension, Math. Ann. **335**, 767 (2006).

[74] D. Bucur and D. Daners, An alternative approach to the Faber-Krahn inequality for Robin problems, Calc. Var. Part. Diff. Eq. **37**, 75 (2010).

[75] M. S. Ashbaugh and R. D. Benguria, Isoperimetric inequalities for eigenvalues of the Laplacian, Proc. Symp. Pure Math. **76**, 105 (2007).

[76] D. S. Grebenkov and B.-T. Nguyen, Geometrical structure of Laplacian eigenfunctions, SIAM Rev. **55**, 601 (2013).

[77] F. Spitzer, Some theorems concerning 2-dimensional Brownian motion, Trans. Am. Math. Soc. **87**, 187 (1958).

[78] G. N. Watson, *A Treatise on the Theory of Bessel Functions* (Cambridge University Press, Cambridge, 1962).

[79] P. E. Levitz, M. Zinsmeister, P. Davidson, D. Constantin, and O. Poncelet, Intermittent Brownian dynamics over a rigid strand: Heavily tailed relocation statistics, Phys. Rev. E **78**, 030102(R) (2008).

[80] O. Bénichou, D. S. Grebenkov, P. Levitz, C. Loverdo, and R. Voituriez, Optimal reaction time for surface-mediated diffusion, Phys. Rev. Lett. **105**, 150606 (2010).

[81] O. Bénichou, C. Loverdo, M. Moreau, and R. Voituriez, Intermittent search strategies, Rev. Mod. Phys. **83**, 81 (2011).

[82] A. V. Chechkin, I. M. Zaid, M. A. Lomholt, I. M. Sokolov, and R. Metzler, Bulk-mediated surface diffusion along a cylinder: Propagators and crossovers, Phys. Rev. E **79**, 040105(R) (2009).

[83] A. V. Chechkin, I. M. Zaid, M. A. Lomholt, I. M. Sokolov, and R. Metzler, Bulk-mediated diffusion on a planar surface: Full solution, Phys. Rev. E **86**, 041101 (2012).

[84] R. Metzler and J. Klafter, The random walk's guide to anomalous diffusion: A fractional dynamics approach, Phys. Rep. **339**, 1 (2000).

[85] R. Metzler and J. Klafter, The restaurant at the end of the random walk: Recent developments in the description of anomalous transport by fractional dynamics, J. Phys. A **37**, R161 (2004).

[86] J. Klafter and I. M. Sokolov, *First Steps in Random Walks: From Tools to Applications* (Oxford University Press, Oxford, 2011).

[87] S. B. Yuste and K. Lindenberg, Subdiffusive target problem: Survival probability, Phys. Rev. E **76**, 051114 (2007).

[88] D. S. Grebenkov, Searching for partially reactive sites: Analytical results for spherical targets, J. Chem. Phys. **132**, 034104 (2010).

[89] D. S. Grebenkov, Subdiffusion in a bounded domain with a partially absorbing-reflecting boundary, Phys. Rev. E **81**, 021128 (2010).

[90] J. D. Eaves and D. R. Reichman, The subdiffusive targeting problem, J. Phys. Chem. B **112**, 4283 (2008).

[91] M. Jeanblanc, M. Yor, and M. Chesney, *Mathematical Methods For Financial Markets* (Springer-Verlag, Berlin, 2009).

[92] D. S. Grebenkov, First exit times of harmonically trapped particles: A didactic review, J. Phys. A **48**, 013001 (2015).

[93] P. E. Levitz, D. S. Grebenkov, M. Zinsmeister, K. Kolwankar, and B. Sapoval, Brownian flights over a fractal nest and first-passage statistics on irregular surfaces, Phys. Rev. Lett. **96**, 180601 (2006).